

# WISE Circumstellar Disks in the Young Sco-Cen Association

A.C. Rizzuto<sup>1</sup>, M.J. Ireland<sup>1,2</sup>, D.B. Zucker<sup>1,2</sup>

<sup>1</sup>*Department of Physics and Astronomy, Macquarie University, Sydney NSW, 2109, Australia*

<sup>2</sup>*Australian Astronomical Observatory, Epping NSW 2121, Australia*

7 November 2018

## ABSTRACT

We present an analysis of the WISE photometric data for 829 stars in the Sco-Cen OB2 association, using the latest high-mass membership probabilities. We detect infrared excesses associated with 135 BAF-type stars, 99 of which are secure Sco-Cen members. There is a clear increase in excess fraction with membership probability, which can be fitted linearly. We infer that  $41 \pm 5\%$  of Sco-Cen OB2 BAF stars to have excesses, while the field star excess fraction is consistent with zero. This is the first time that the probability of non-membership has been used in the calculation of excess fractions for young stars. We do not observe any significant change in excess fraction between the three subgroups. Within our sample, we have observed that B-type association members have a significantly smaller excess fraction than A and F-type association members.

**Key words:** circumstellar matter - open clusters and associations: individual (Sco-Cen, Sco OB2) - protoplanetary disks - planets and satellites: formation - stars: early-type.

## 1 INTRODUCTION

Many young ( $\sim 1$ -10 Myr) stars of all types, ranging from tens of solar masses down to the smallest brown dwarves and in all environments, are surrounded by circumstellar disks (Strom et al. 1989; Lada et al. 2000; Carpenter et al. 2006). A variety of observations have provided us with an overall timeline of disk evolution. The inner portion of the disk ( $\leq 1$  AU) dissipates by the age of 10 Myr in all but a small fraction of stars (Mamajek et al. 2004; Silverstone et al. 2006). From the age of 10 Myr onwards, there is an observed decline in the  $24\mu$ m excess relative to the photosphere for stars of B to K type (Gáspár et al. 2009; Rieke et al. 2005). It has been postulated that planetesimal stirring through stellar ages of 5 to 20 Myr could produce an increase in the strength of the  $\sim 24\mu$ m excess with age (Kenyon & Bromley 2008), however the current data do not show a statistically significant increase (Carpenter et al. 2009).

The Sco-Cen association and its three subgroups—Upper Scorpius (US), Upper Centaurus Lupus (UCL) and Lower Centaurus Crux (LCC)—provide three important constant-age samples within which to study circumstellar disks around young stars. The subgroups have ages of  $\sim 5$ ,  $\sim 16$ , and  $\sim 17$  Myr respectively, and are located less than 150 pc from the Sun (de Zeeuw et al. 1999). Previous studies (Carpenter et al. 2006, 2009) have investigated IRAC, IRS and Spitzer photometric data ranging from 4.5 to  $70\mu$ m in the US subgroup. They identified 54 stars with  $24\mu$ m excesses

in their sample of 205 targets and found that disks around BAF-type stars appear to be comprised of dusty debris, while disks associated with K and M-type stars are likely optically thick primordial disks which are remnants of the star formation process. The older Sco-Cen subgroups, UCL and LCC have received considerably less attention; only a handful of studies have observed small numbers of UCL and LCC stars (Su et al. 2006; Carpenter et al. 2009). The recent study by Chen et al. (2011) reports the detection of 41 new disks around F and G-type Sco-Cen stars.

New Bayesian membership probabilities for the high mass members (B to F-type) of the Sco-Cen association are now available (Rizzuto et al. 2011), and preliminary photometric data from the WISE mission have been released (Wright et al. 2010). In this paper we present an analysis of the WISE photometry for Sco-Cen members to search for circumstellar disks in three constant-age samples.

## 2 DATA SAMPLE

In this study we take our sample from the Hipparcos Sco-Cen membership study of Rizzuto et al. (2011). All stars with membership probabilities of 5% and greater were cross-referenced with the WISE preliminary data release. This resulted in a sample of 829 stars with spectral types ranging from early B to late F ( $B-V \leq 0.6$ ), brighter than  $9^{th}$  visual magnitude and within the area of sky bounded by

( $285 \leq l \leq 360$ ) and ( $-10 \leq b \leq 60$ ). Taking into consideration membership probabilities, this equates to  $\sim 400$  true members. Membership as described in Rizzuto et al. (2011) is based purely on kinematic and positional properties of the targets, and hence the selection is believed to be unbiased with regard to the presence of circumstellar disks. We have chosen to include the low membership probability stars in this study in order to use a potential relationship between excess fraction and probability of membership to infer a more accurate excess fraction for secure members.

### 3 WISE EXCESSES

The WISE mission data provides photometry in four bands,  $W_1$ ,  $W_2$ ,  $W_3$  and  $W_4$ , with central wavelengths of 3, 4.5, 12 and  $22\mu m$  respectively (Wright et al. 2010). In this study we present an analysis of three WISE colours:  $W_1-W_2$ ,  $W_1-W_3$ , and  $W_1-W_4$ . Inspection of the WISE photometry for band  $W_2$  shows a clear bias at the bluest end of our membership sample towards poorly fitted point-spread-functions, resulting in untrustworthy  $W_2$  photometry. For this reason the long wavelength colours were constructed with  $W_1$ , which shows a uniform distribution across spectral type of poor photometry fits. Analysis of these three colours will provide three different classes of detected excesses: (1) excesses in all colours, (2) excesses in only the short wavelength filters, and (3) excess in only the longer or longest wavelengths. It is expected that a disk-produced excess detected at bluer colours will also be detected at longer colours, hence, excesses in only the blue colours will indicate contaminated photometry.

Stellar photospheric emission is expected to vary linear with 2MASS ( $J-K_s$ ) colour. To determine the photospheric colours, we have applied an iterative fitting procedure. Objects which were clear outliers in the particular WISE colour were first removed and then the software package MPFIT was used to fit a line to the sample. Objects separated from the fitted line by more than twice the dispersion of the residuals were then removed as outliers. The process was then repeated until no further objects were removed. This fitting procedure was carried out using only the stars with greater than 60% membership probability in order to ensure that the fitted photosphere line was that of the young Sco-Cen stars. During this fitting procedure, objects with a WISE photometric fit reduced  $\chi^2$  greater than 4 in the relevant bands were excluded, as they are likely to be extended sources with poor photometry.

The criterion adopted for excess detection in the three colours was 8% for  $W_1-W_2$ , 13% for  $W_1-W_3$  and 30% for  $W_1-W_4$  above the expected photosphere line, plus the error on the WISE photometry. These detection thresholds were chosen conservatively such that the detections are likely to be significant even if the photosphere fit is underestimated by 10%. The colour-colour diagrams for the three WISE colours and the fits can be seen in Figure 1.

Given excess detections in the three WISE colours we can remove from the sample those stars with suspect photometry. There were 19 objects with a detected excess in  $W_1-W_2$  only, 3 in  $W_1-W_3$  only, and 3 in  $W_1-W_2$  and  $W_1-W_4$  only. The 19 objects which show an excess only in the  $W_1-W_2$  colour are likely caused by the saturation be-

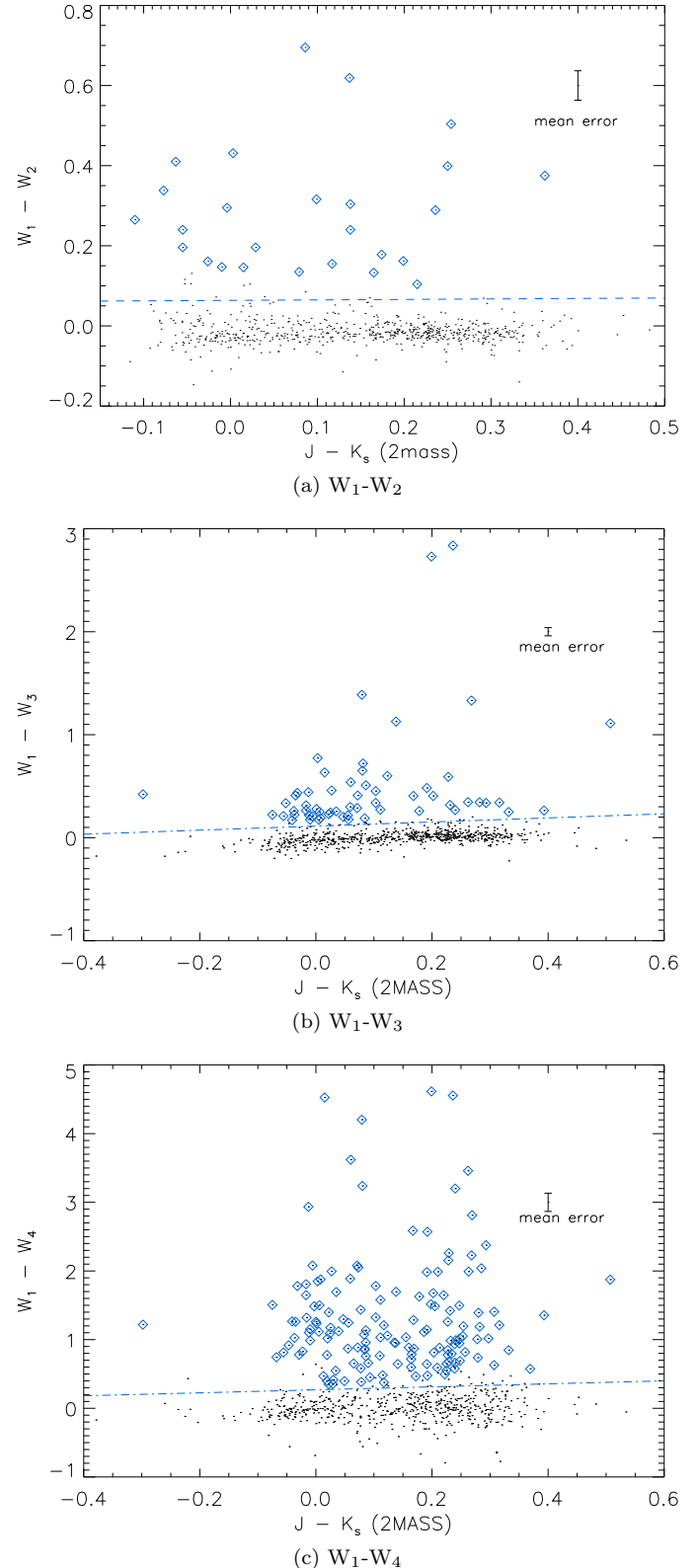


**Figure 1.** The colour-colour diagrams for the three WISE colours defined above. The blue line represents the corresponding excess detection threshold above which objects are considered to have a detectable excess. The photosphere grouping is clearly seen in each colour with fitted slopes and intercepts of  $(0.012, -0.18)$ ,  $(0.019, -0.018)$  and  $(0.22, -0.016)$  respectively. Blue diamonds indicate stars with detectable excesses.

haviour of the WISE photometry fits. When partial saturation occurs in band  $W_2$  (brighter than 6.5 mags), the WISE photometry fitting procedure produces a systematic overestimation of the flux (Cutri et al. 2011). All 19 of these objects are in the  $W_2$  magnitude range where flux overestimation is expected and hence we have treated these objects in our sample as having no detectable excess. In addition, we remove those objects with poor photometry fits ( $\chi^2 > 4$ ) in the  $W_1$  and  $W_4$  bands, as the remainder of the analysis makes use of the  $W_1$ - $W_4$  excess only; there were 95 such objects. HIP 77562 and 81891, which only show an excess in  $W_1$ - $W_3$  both have poor photometry fits in band  $W_4$ , and so are removed from the sample. HIP 77911 shows a poor photometry fit in the  $W_1$  band ( $\chi^2 = 4.6$ ), which is only marginally above our cut ( $\chi^2 = 4$ ). HIP 77911 also shows a strong excess in the  $W_2$ - $W_4$  colour, where the photometry fits are reliable, and hence we have included HIP 77911 in our sample with a  $22\mu\text{m}$  excess.

The WISE images of the 173 objects with detected excesses were then visually inspected for the presence of close, unresolved companions and contamination from excess-producing nebulosity. This yielded 27 objects with excesses not likely to be caused by a disk. HIP 68413, 79098 and 76063, which have detectable excess in  $W_1$ - $W_2$  and  $W_1$ - $W_4$ , but not  $W_1$ - $W_3$ , are included in the sample based on the image inspection. The lack of  $W_1$ - $W_3$  excess associated with HIP 68413 is most likely due to a large error on  $W_1$ - $W_3$  and the detected  $W_1$ - $W_2$  excess associated with HIP 79098 was found to be caused by a clearly visible diffraction spike in the  $W_2$  image. HIP 76063 has a  $W_2$  magnitude of 5.6, and so the  $W_1$ - $W_2$  excess associated with this star is most likely due to saturation. Finally, HIP 80897 shows a nebulous excess in  $W_1$ - $W_3$  only, and so was removed from the sample. In total, we observe reliable excesses associated with 135 objects: 28 stars in US, 53 in UCL and 54 in LCC.

## 4 DISCUSSION

The sources investigated in this study are BAF-type stars and hence the detected excesses are expected to be produced by dusty debris disks rather than primordial gaseous disks (Carpenter et al. 2009). A clear outcome of our analysis is that the excess fraction in the three subgroups is not uniform with respect to membership probability ( $p$ ). Figure 2 displays the excess fraction in 10% membership probability bins with  $p > 20\%$ . We have fitted linear trends to these data. Extrapolation to 100% membership probability (i.e. certain members) along the linear fits results in excess fractions of  $0.38 \pm 0.1$ ,  $0.33 \pm 0.08$  and  $0.46 \pm 0.13$  for the three subgroups.

The extrapolated excess fraction for US is larger than the observed  $24\mu\text{m}$  excess fraction in the US sample used by Carpenter et al. (2009), which was found to be  $\sim 0.3$  for B7-A9 stars and  $\sim 0.15$  for F-type stars, and is in agreement with the value of  $\sim 0.33$  for F and G-type US stars seen by Chen et al. (2011). For associations at the age of UCL and LCC (16, 17 Myr), Chen et al. (2005) reported a  $24\mu\text{m}$  excess fraction lower-bound of  $\sim 0.35$ , and Rieke et al. (2005) and Su et al. (2006) observe that 60% of young stars ( $< 30$  Myr) do not have an excess. These results are consistent with our study. We do not see an increase in the

$22\mu\text{m}$  excess fraction for the two older subgroups (UCL, LCC). Previous observations have provided some evidence for a peak in the excess fraction as stars age from  $< 10$  Myr to the 10-30 Myr age range (Currie et al. 2008; Gáspár et al. 2009). However, our analysis shows that in the Sco-Cen association, the excess fraction does not change significantly between the three subgroups. A recent study (Pecaut et al. 2011) suggests that the true age of US may in fact be  $\sim 11$  Myr, which offers a potential explanation for the lack of an excess fraction increase between the subgroups.

Given the lack of statistically significant differences in excess fraction between the three Sco-Cen subgroups, the association as a whole can be explored. Figure 2d displays the linear excess fraction trend for combined sample. The extrapolated excess fraction was  $41 \pm 5\%$  for certain members, and consistent with 0% for field stars, with a  $\chi^2$  of 1.3 for the fit.

We have cross checked our sample with those of the Spitzer MIPS studies of Chen et al. (2011), Carpenter et al. (2009), Su et al. (2006), and Chen et al. (2005) as a basic assessment of the relative success of the WISE photometry in identifying excesses. We see that of those stars in both data sets which passed our photometry tests, six have observed excesses above 30% in the MIPS sample but are not assigned an excess in our study. Of these six stars, five have measured  $22\mu\text{m}$  flux as a multiple of the photosphere within one-sigma of the corresponding MIPS  $24\mu\text{m}$  values. The remaining star, HIP 79673, has a WISE flux ratio of  $1.23 \pm 0.15$ , while the MIPS value is  $1.53 \pm 0.05$ . Chen et al. (2011) indicate that the MIPS photometry for this star is contaminated, and the WISE image shows significant contamination in the form of well-resolved extended emission. This is most likely the cause of the discrepancy. Furthermore, there are two sources with large MIPS flux ratios (5-10 times the photosphere) which did not pass our photometry tests. HIP 61087 has very poor WISE photometry fits as well as clear contamination in the images (and in the MIPS data), though the measured flux ratio is similar to that of Chen et al. (2011). The presence of an excess cannot be made clear from the data and so no further comments on this object can be made. Finally, HIP 80921 shows a relatively strong excess, however inspection of the images clearly show that the excess is caused by extended emission. Similarly, the Spitzer MIPS images show extended emission with no clear stellar source at  $24\mu\text{m}$ .

The correlation between the presence of a circumstellar disk and membership of the Sco-Cen association is clearly demonstrated in this analysis. It is thus important to consider stars with a detectable  $22\mu\text{m}$  excess which have lower membership probabilities ( $p < 50\%$ ). In the latest Sco-Cen membership study (Rizzuto et al. 2011) a number of de Zeeuw et al. (1999) member stars were assigned low membership probabilities due to inconclusive proper motion data and the lack of a radial velocity measurement. Unresolved multiplicity has long been recognised as an important pitfall in kinematics-based association membership selection methods. An equal mass binary system at the distance of Sco-Cen can produce a proper-motion offset on the order of  $\sim 2$  mas from the true centre-of-mass motion. This is approximately the size of the uncertainties in the proper motion (van Leeuwen 2007), indicating that binary association members can be overlooked. The presence of a circumstel-

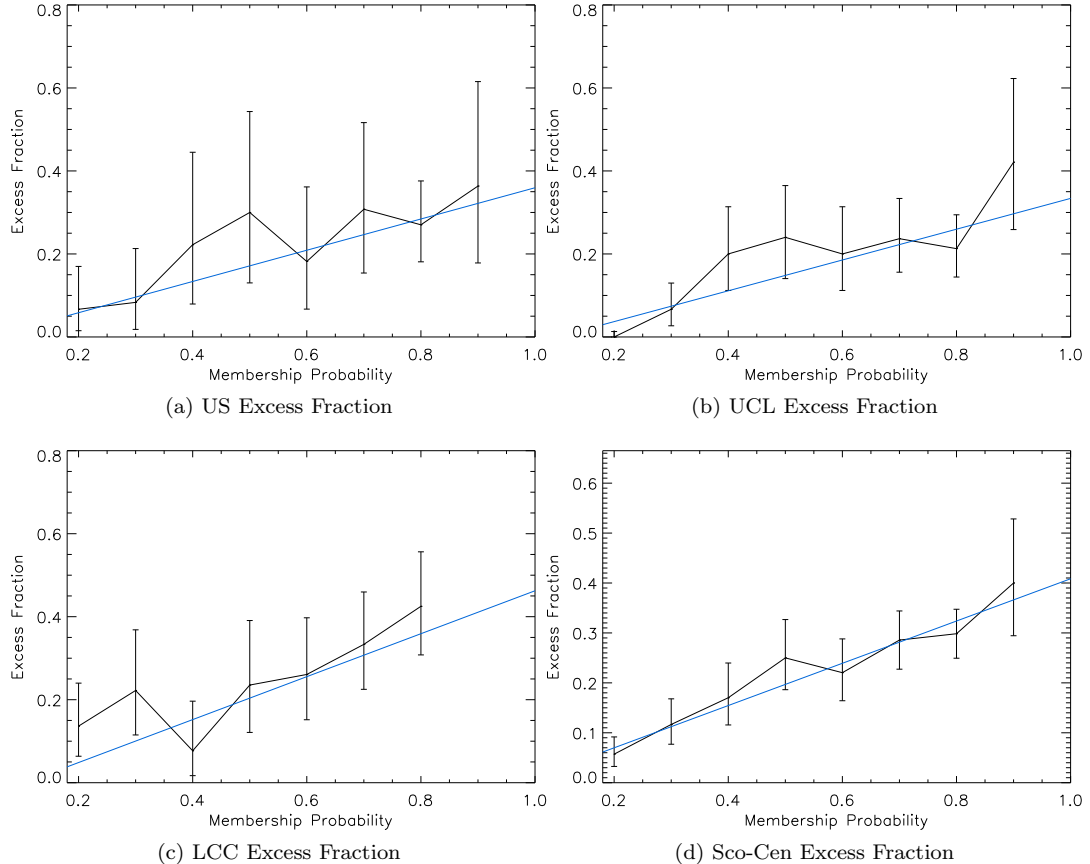


**Figure 2.** Excess fraction as a function of membership probability for the three subgroups and the entire association.

HIP	P	$F_{W_4}$	$\sigma_{F_{W_4}}$	$R(W_2)$	$\sigma_{R(W_2)}$	$R(W_3)$	$\sigma_{R(W_3)}$	$R(W_4)$	$\sigma_{R(W_4)}$	Excess <sup>a</sup>	Subgroup
49360	6	12.02	0.76	0.99	0.03	0.98	0.03	1.03	0.07	NNN	LCC
50612	7	14.02	0.80	0.99	0.03	1.05	0.03	1.46	0.09	NNY	LCC
50667	7	11.54	0.71	1.01	0.03	1.23	0.04	2.24	0.15	NYY	LCC

**Table 1. N.B.** Complete table online. The and WISE band fluxes as a multiple of the photosphere calculated from the three WISE colours and the 22  $\mu$ m flux. <sup>a</sup> This column indicates the detection of an excess in the three colours. The fluxes are in mJy.

lar disk can then be used to indicate membership for stars spatially and photometrically consistent, but kinematically inconsistent, with the Sco-Cen subgroups. We thus increase the Bayes' factors (see Rizzuto et al. 2011) of stars with between 10% and 50% membership probability and a detected excess by a conservative factor of 4.8 (Table 2). This is the lower bound of the 99% confidence interval of the ratio of excess fractions at 100% and 0% membership probability. Note that including these stars in a sample of Sco-Cen members will necessarily introduce a bias toward disk presence.

The subgroup LCC has an anomalous concentration of stars with detectable excess in the 5–10% membership probability range. Three of these stars, HIP 50612, 52867 and 53992, are known members of the young open cluster IC2602, which is on the far side of LCC (Robichon et al. 1999), and are thus expected to have low Sco-Cen membership probabilities. Confusion with young background sources for this subgroup, which is on the Galactic plane, further contributes to the anomalous high excess fraction.

HIP	P	HIP	P	HIP	P	HIP	P
51169	57	51203	71	53524	81	55616	46
60183	69	62482	59	62488	72	63236	76
63395	58	72099	81	76223	81	76782	75
77315	80	77523	70	78198	76	78357	49
78826	79	78943	82	80019	64	80458	82
81316	77	82154	48	83232	36	84881	43
86853	50						

**Table 2.** The 25 excess detections around low probability members and the adjusted probabilities.

We have examined the excess fraction properties of our sample in three colour ranges: ( $-0.3 < B-V < 0$ ), ( $0 < B-V < 0.3$ ) and ( $0.3 < B-V < 0.6$ ). These groupings correspond approximately to B, A and F-type stars according to the colour tables of Allen & Cox (2000). Figure 3 displays plots of the excess fraction against membership probability for

Figure	a	b	Corr	$\chi^2$
US	0.38±0.10	-0.02±0.09	-0.65	0.6
UCL	0.33±0.08	-0.04±0.06	-0.68	2.2
LCC	0.46±0.13	-0.05±0.11	-0.77	3.3
All	0.41±0.05	-0.02±0.04	-0.65	1.3
B	0.18±0.10	0.09±0.10	-0.73	0.5
A	0.45±0.11	0.05±0.09	-0.61	2.2
F	0.47±0.09	-0.08±0.04	-0.77	2.8

**Table 3.** The excess fraction fits for the seven graphs. The fitting was done to the equation  $y = (a - b)p_{mem} + b$ , where a and b are the excess fractions at  $p_{mem} = 1.0$  and 0 respectively.

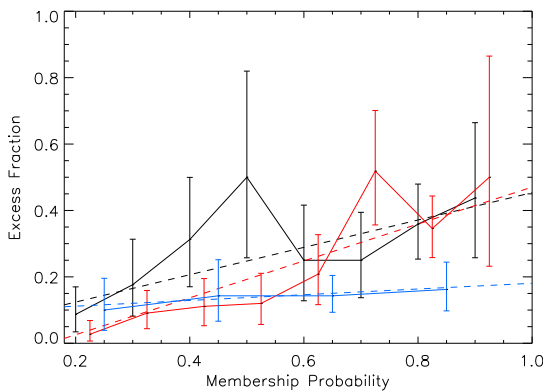


**Figure 3.** Excess fraction against membership probability for A-type (Black), F-type (Red) and B-type (Blue) stars in our sample. The dashed lines represent the linear fits.

the three spectral type ranges. We find the extrapolated excess fractions for the A and F-type stars to be  $45\pm11\%$  and  $47\pm9\%$ , while the B-type stars in our sample show no evidence of a trend in excess fraction with membership probability. The study of Carpenter et al. (2009) also found that A and F-type stars have similar excess fractions at the age of Sco-Cen, with a small increase in excess fraction for the earlier spectral types. However, the earliest star included in the Carpenter et al. (2009) sample is B7, and so no direct comparison can be made to the bluest end of our sample.

## 5 SUMMARY AND CONCLUSIONS

We have analysed the available preliminary WISE photometry for the Sco-Cen stars of the Rizzuto et al. (2011) membership list and detected 135  $22\mu\text{m}$  excesses above the expected photosphere emission. We have used Sco-Cen membership probabilities to extrapolate an excess fraction for certain members, and observe that there is no significant difference in excess fraction between the three association subgroups. This agrees with previous studies (Carpenter et al. 2009) and may be explained by the revised US age of  $\sim 11$  Myr (Pecaut et al. 2011). Importantly we find that the excess fraction is significantly lower for the B-type stars in our sample compared to A and F-type association members, which is contrary to the trend seen by Carpenter et al. (2009). It is possible that the lack of a clear trend for the B-type sample could indicate that most of them are in fact young Sco-Cen members despite their kinematics. Another

possible explanation relates to multiplicity. B-type stars have a significantly higher multiplicity fraction compared to later type stars (Kouwenhoven et al. 2005). The presence of a companion can potentially truncate the inner regions of the circumstellar disk through resonances (Artymowicz & Lubow 1994), producing a smaller disk fraction. This has been observed in a recent study of binaries in Taurus-Auriga, particularly with close ( $<40$  AU) companions (Kraus et al. 2011). Among the highest probability members in our sample ( $>90\%$ ) there are six close ( $<100$  AU) multiple systems without disk detections and one close multiple system with a detected excess. A closer, more comprehensive, comparison between disk presence and multiplicity information for the Sco-Cen B-type stars may shed light on this issue, but is beyond the scope of this study.

## REFERENCES

- Allen C., Cox A., 2000, Allen's astrophysical quantities. AIP Press
- Artymowicz P., Lubow S. H., 1994, ApJ, 421, 651
- Carpenter J. M., Mamajek E. E., Hillenbrand L. A., Meyer M. R., 2006, ApJ, 651, L49
- , 2009, ApJ, 705, 1646
- Chen C. H., Jura M., Gordon K. D., Blaylock M., 2005, ApJ, 623, 493
- Chen C. H., Mamajek E. E., Bitner M. A., Pecaut M., Su K. Y. L., Weinberger A. J., 2011, ApJ, 738, 122
- Currie T., Plavchan P., Kenyon S. J., 2008, ApJ, 688, 597
- Cutri R. M. et al., 2011, Explanatory Supplement to the WISE Preliminary Data Release Products. Tech. rep.
- de Zeeuw P. T., Hoogerwerf R., de Bruijne J. H. J., Brown A. G. A., Blaauw A., 1999, AJ, 117, 354
- Gáspár A., Rieke G. H., Su K. Y. L., Balog Z., Trilling D., Muzzarelli J., Apai D., Kelly B. C., 2009, ApJ, 697, 1578
- Kenyon S. J., Bromley B. C., 2008, ApJS, 179, 451
- Kouwenhoven M. B. N., Brown A. G. A., Zinnecker H., Kaper L., Portegies Zwart S. F., 2005, A&A, 430, 137
- Kraus A. L., Ireland M. J., Hillenbrand L. A., Martinache F., 2011, ArXiv e-prints
- Lada C. J., Muench A. A., Haisch Jr. K. E., Lada E. A., Alves J. F., Tollestrup E. V., Willner S. P., 2000, AJ, 120, 3162
- Mamajek E. E., Meyer M. R., Hinz P. M., Hoffmann W. F., Cohen M., Hora J. L., 2004, ApJ, 612, 496
- Pecaut M. J., Mamajek E. E., Bubar E. J., 2011, ArXiv e-prints
- Rieke G. H. et al., 2005, ApJ, 620, 1010
- Rizzuto A. C., Ireland M. J., Robertson J. G., 2011, MNRAS, 416, 3108
- Robichon N., Arenou F., Mermilliod J.-C., Turon C., 1999, A&A, 345, 471
- Silverstone M. D. et al., 2006, ApJ, 639, 1138
- Strom K. M., Strom S. E., Edwards S., Cabrit S., Skrutskie M. F., 1989, AJ, 97, 1451
- Su K. Y. L. et al., 2006, ApJ, 653, 675
- van Leeuwen F., ed., 2007, Astrophysics and Space Science Library, Vol. 350, Hipparcos, the New Reduction of the Raw Data
- Wright E. L. et al., 2010, AJ, 140, 1868

Table 4: The WISE band 4 flux and  $W_2, W_3$  and  $W_4$  flux as a multiple of the photosphere with errors for our sample. <sup>a</sup> This column indicates the detection of an excess in the three colours. The lower section of the table displays the objects removed from our sample due to poor photometry or unreliable images.

HIP	P	$F_{W_4}$ (mJy)	$\sigma_{F_{W_4}}$ (mJy)	R( $W_2$ )	$\sigma_{R(W_2)}$	R( $W_3$ )	$\sigma_{R(W_3)}$	R( $W_4$ )	$\sigma_{R(W_4)}$	Excess <sup>a</sup>	Subgroup
49360	6	12.02	0.76	0.99	0.03	0.98	0.03	1.03	0.07	NNN	LCC
50612	7	14.02	0.80	0.99	0.03	1.05	0.03	1.46	0.09	NNY	LCC
50667	7	11.54	0.71	1.01	0.03	1.23	0.04	2.24	0.15	NYY	LCC
51169	22	8.61	0.72	1.00	0.03	1.25	0.04	2.17	0.19	NYY	LCC
51203	33	9.97	0.74	0.99	0.03	1.06	0.03	1.55	0.12	NNY	LCC
51507	9	11.47	0.92	1.02	0.02	0.98	0.02	0.90	0.07	NNN	LCC
51508	6	12.72	0.82	0.97	0.03	0.97	0.03	1.04	0.07	NNN	LCC
52059	6	13.41	0.85	0.98	0.03	0.99	0.03	0.94	0.07	NNN	LCC
52116	7	15.55	0.79	0.97	0.03	0.96	0.03	0.93	0.05	NNN	LCC
52132	13	8.42	0.71	1.00	0.03	1.01	0.03	0.98	0.09	NNN	LCC
52293	15	15.74	0.83	0.97	0.03	0.99	0.04	1.01	0.06	NNN	LCC
52357	82	15.33	0.86	1.00	0.04	0.98	0.03	0.90	0.06	NNN	LCC
52867	8	16.99	0.97	1.00	0.03	1.15	0.03	2.68	0.17	NNY	LCC
53016	7	9.47	0.78	1.00	0.03	1.00	0.03	0.98	0.08	NNN	LCC
53524	46	51.60	1.47	0.98	0.04	1.05	0.04	3.02	0.13	NNY	LCC
53913	7	10.34	0.81	1.02	0.03	1.04	0.03	1.11	0.09	NNN	LCC
53992	9	12.40	0.90	1.00	0.03	1.01	0.03	2.54	0.19	NNY	LCC
54176	40	6.47	0.95	1.01	0.03	1.01	0.03	0.97	0.15	NNN	LCC
55205	11	2.88	0.92	1.01	0.03	0.98	0.04	0.74	0.24	NNN	LCC
55334	58	12.17	0.81	1.02	0.03	1.01	0.03	0.95	0.07	NNN	LCC
55616	15	20.19	1.02	0.99	0.03	1.18	0.03	3.16	0.17	NNY	LCC
56227	58	6.99	0.74	0.98	0.03	0.97	0.03	0.88	0.10	NNN	LCC
56354	84	27405.65	403.86	4.02	0.25	16.99	0.94	203.00	11.43	NNY	LCC
56561	24	443.65	12.26	2.17	0.12	1.01	0.06	0.98	0.06	NNN	LCC
56993	33	8.77	0.81	1.00	0.03	1.01	0.03	0.95	0.09	NNN	LCC
57043	6	7.44	0.65	0.98	0.03	0.97	0.03	0.90	0.08	NNN	LCC
57238	26	5.03	0.79	0.95	0.02	0.99	0.03	1.20	0.19	NNN	LCC
57273	5	4.26	0.79	1.00	0.03	0.99	0.03	1.21	0.22	NNN	LCC
57285	46	12.24	0.94	1.00	0.03	0.97	0.03	1.23	0.10	NNN	LCC
57375	51	11.25	0.91	1.03	0.03	1.03	0.03	1.05	0.09	NNN	LCC
57531	7	7.08	0.65	1.00	0.03	1.00	0.03	1.06	0.10	NNN	LCC
57644	21	17.12	0.98	0.99	0.04	1.00	0.04	1.11	0.07	NNN	LCC
57669	9	413.28	8.75	1.96	0.14	1.73	0.11	2.63	0.17	NNY	LCC
57851	73	64.60	1.84	1.21	0.07	0.94	0.05	0.98	0.06	NNN	LCC
57947	50	13.96	0.87	1.02	0.03	1.00	0.03	0.99	0.07	NNN	LCC
57950	76	19.87	1.32	1.01	0.03	1.04	0.03	1.77	0.13	NNY	LCC
57953	26	2.21	0.89	0.99	0.03	0.97	0.03	0.78	0.32	NNN	LCC
58054	34	5.84	0.86	0.98	0.03	1.00	0.03	1.01	0.15	NNN	LCC
58075	47	7.10	0.84	0.95	0.02	0.95	0.02	1.07	0.13	NNN	LCC
58146	77	15.84	1.15	0.99	0.04	0.96	0.03	0.92	0.07	NNN	LCC
58167	87	11.63	0.87	1.00	0.03	1.00	0.03	1.07	0.08	NNN	LCC
58220	88	28.30	1.23	1.02	0.03	1.33	0.04	2.86	0.14	NNY	LCC
58416	87	17.92	0.96	1.04	0.04	1.01	0.04	1.08	0.07	NNN	LCC
58465	88	25.69	1.06	1.05	0.04	1.00	0.04	1.02	0.05	NNN	LCC
58670	11	5.15	0.72	0.99	0.03	0.99	0.03	0.87	0.12	NNN	LCC
58680	48	2.49	0.81	0.98	0.03	0.97	0.03	0.67	0.22	NNN	LCC
58720	59	118.75	2.62	1.05	0.04	1.27	0.05	4.12	0.18	NNY	LCC
58760	21	7.98	0.84	1.00	0.03	1.03	0.04	1.08	0.12	NNN	LCC
58859	83	19.47	1.02	1.00	0.04	0.98	0.04	0.99	0.06	NNN	LCC
58884	78	57.68	1.49	1.34	0.07	1.01	0.05	1.00	0.05	NNN	LCC
58899	84	9.07	0.86	1.01	0.03	0.97	0.03	0.82	0.08	NNN	LCC
58901	51	21.41	2.07	1.01	0.04	0.96	0.04	0.84	0.09	NNN	LCC
59084	23	3.45	1.33	0.97	0.03	0.93	0.03	0.47	0.18	NNN	LCC
59173	66	84.61	3.20	1.61	0.09	0.98	0.05	0.97	0.06	YNN	LCC
59184	40	65.32	1.99	1.34	0.08	0.96	0.05	0.98	0.06	YNN	LCC
59281	26	12.40	0.75	1.01	0.03	0.99	0.03	0.94	0.06	NNN	LCC

Table 4: The WISE band 4 flux and  $W_2, W_3$  and  $W_4$  flux as a multiple of the photosphere with errors for our sample. <sup>a</sup> This column indicates the detection of an excess in the three colours. The lower section of the table displays the objects removed from our sample due to poor photometry or unreliable images.

HIP	P	$F_{W_4}$ (mJy)	$\sigma_{F_{W_4}}$ (mJy)	$R(W_2)$	$\sigma_{R(W_2)}$	$R(W_3)$	$\sigma_{R(W_3)}$	$R(W_4)$	$\sigma_{R(W_4)}$	Excess <sup>a</sup>	Subgroup
59282	88	28.70	1.14	1.03	0.03	1.19	0.04	2.21	0.11	NYY	LCC
59383	6	2.70	0.87	0.99	0.03	0.98	0.03	0.91	0.30	NNN	LCC
59397	86	42.64	1.34	1.02	0.04	1.21	0.04	3.32	0.14	NYY	LCC
59430	30	4.57	0.69	0.99	0.03	0.96	0.03	0.82	0.13	NNN	LCC
59449	60	124.01	2.74	1.80	0.11	1.07	0.06	1.05	0.06	NNN	LCC
59481	88	8.76	1.02	0.97	0.03	0.99	0.03	0.99	0.12	NNN	LCC
59502	86	100.98	4.37	1.03	0.04	1.54	0.06	6.34	0.33	NYY	LCC
59505	81	5.78	0.85	1.03	0.03	1.04	0.03	0.81	0.12	NNN	LCC
59541	33	13.75	1.04	1.02	0.03	1.02	0.03	1.07	0.09	NNN	LCC
59579	13	4.50	0.90	0.99	0.03	0.98	0.03	0.79	0.16	NNN	LCC
59603	82	10.22	0.84	1.03	0.03	1.00	0.03	1.10	0.09	NNN	LCC
59693	74	9.18	0.92	1.01	0.03	1.20	0.04	2.07	0.21	NYY	LCC
59716	64	12.77	1.01	0.99	0.03	1.00	0.03	1.15	0.10	NNN	LCC
59724	59	39.14	1.37	1.00	0.03	1.14	0.03	4.25	0.18	NNY	LCC
59747	75	283.82	6.80	1.69	0.12	0.99	0.07	0.87	0.06	NNN	LCC
59897	28	3.08	0.91	1.00	0.03	1.04	0.03	1.03	0.31	NNN	LCC
59960	89	108.90	2.91	1.00	0.04	1.07	0.04	6.02	0.24	NNY	LCC
60009	79	119.52	2.97	1.32	0.08	0.93	0.05	0.98	0.06	NNN	LCC
60084	42	9.29	0.91	0.99	0.03	1.03	0.03	1.15	0.12	NNN	LCC
60183	31	106.23	2.35	1.09	0.04	1.36	0.05	4.65	0.19	NYY	LCC
60205	62	3.16	0.88	0.98	0.03	1.01	0.03	1.18	0.33	NNN	LCC
60245	74	5.53	0.82	1.06	0.02	1.07	0.03	1.03	0.16	NNN	LCC
60348	78	14.29	1.03	1.01	0.03	1.06	0.03	1.89	0.14	NNY	LCC
60360	44	9.10	0.89	1.00	0.03	1.02	0.03	1.12	0.11	NNN	LCC
60379	53	39.80	4.58	1.15	0.13	1.04	0.10	1.02	0.15	NNN	LCC
60459	88	14.74	1.13	1.03	0.04	1.03	0.04	1.14	0.09	NNN	LCC
60513	76	7.02	0.91	1.01	0.03	0.97	0.03	0.79	0.10	NNN	LCC
60561	73	48.29	1.29	1.03	0.04	1.26	0.05	2.63	0.11	NYY	LCC
60577	81	18.22	1.09	0.98	0.03	1.00	0.03	1.35	0.09	NNN	LCC
60580	5	8.88	0.78	0.99	0.03	0.98	0.03	1.09	0.10	NNN	LCC
60629	6	1.71	0.68	0.98	0.03	0.99	0.03	0.61	0.24	NNN	LCC
60710	71	60.90	2.47	1.38	0.08	0.98	0.05	0.98	0.07	NNN	LCC
60823	79	115.52	2.66	1.84	0.11	1.04	0.06	1.02	0.06	NNN	LCC
60851	82	37.41	2.17	1.06	0.05	0.99	0.04	1.12	0.08	NNN	LCC
60855	70	47.80	1.54	1.18	0.06	1.02	0.05	1.04	0.06	YNN	LCC
61049	85	45.86	1.39	0.97	0.03	1.21	0.04	3.27	0.13	NYY	LCC
61086	20	1.71	0.81	1.00	0.03	1.03	0.04	1.42	0.68	NNN	LCC
61098	8	3.82	0.83	1.00	0.03	1.03	0.03	1.00	0.22	NNN	LCC
61257	84	18.96	0.94	1.03	0.04	1.02	0.04	1.05	0.06	NNN	LCC
61265	67	9.57	0.88	1.00	0.03	1.00	0.03	1.04	0.10	NNN	LCC
61268	26	3.23	0.62	1.00	0.03	1.02	0.03	0.80	0.15	NNN	LCC
61426	54	7.74	0.97	1.00	0.03	1.02	0.03	1.10	0.14	NNN	LCC
61498	81	2517.91	20.87	1.12	0.06	1.82	0.09	65.43	3.00	NYY	LCC
61530	24	3.90	0.78	0.99	0.03	1.01	0.03	0.87	0.17	NNN	LCC
61557	34	30.13	1.36	1.05	0.04	0.98	0.04	1.01	0.06	NNN	LCC
61585	71	327.37	13.87	1.54	0.10	0.86	0.06	0.83	0.07	NNN	LCC
61639	84	28.59	1.19	0.96	0.04	0.94	0.04	0.97	0.05	NNN	LCC
61684	73	44.94	1.45	0.99	0.03	1.11	0.04	3.83	0.16	NNY	LCC
61691	14	2.50	0.85	1.02	0.03	1.04	0.03	0.82	0.28	NNN	LCC
61715	8	30.19	5.53	0.95	0.03	1.51	0.09	5.13	0.95	NYY	LCC
61717	21	4.92	1.04	1.00	0.03	1.01	0.03	1.31	0.28	NNN	LCC
61753	13	14.22	0.98	0.99	0.03	0.98	0.03	1.29	0.09	NNN	LCC
61782	84	218.09	4.82	1.01	0.03	1.65	0.05	28.15	0.92	NYY	LCC
61789	15	95.55	2.55	1.52	0.11	0.95	0.06	0.97	0.07	NNN	LCC
61796	61	21.75	0.88	1.02	0.04	0.99	0.04	0.96	0.05	NNN	LCC
61845	12	3.06	0.70	0.99	0.03	0.99	0.03	0.97	0.22	NNN	LCC

Table 4: The WISE band 4 flux and  $W_2, W_3$  and  $W_4$  flux as a multiple of the photosphere with errors for our sample. <sup>a</sup> This column indicates the detection of an excess in the three colours. The lower section of the table displays the objects removed from our sample due to poor photometry or unreliable images.

HIP	P	$F_{W_4}$ (mJy)	$\sigma_{F_{W_4}}$ (mJy)	R( $W_2$ )	$\sigma_{R(W_2)}$	R( $W_3$ )	$\sigma_{R(W_3)}$	R( $W_4$ )	$\sigma_{R(W_4)}$	Excess <sup>a</sup>	Subgroup
61906	40	4.19	0.77	0.99	0.03	0.97	0.03	0.80	0.15	NNN	LCC
62026	77	40.80	1.35	1.05	0.05	1.06	0.05	1.26	0.07	NNN	LCC
62032	73	7.03	0.84	1.07	0.03	1.11	0.03	1.21	0.14	NNN	LCC
62058	80	27.61	1.14	0.98	0.05	0.94	0.04	0.98	0.06	NNN	LCC
62085	6	3.36	0.81	0.98	0.03	1.01	0.03	1.12	0.27	NNN	LCC
62087	11	10.38	0.92	0.97	0.03	0.97	0.03	1.03	0.09	NNN	LCC
62154	39	7.81	3.74	1.00	0.03	1.08	0.10	1.56	0.75	NNN	LCC
62171	78	7.45	0.87	1.01	0.03	0.99	0.03	1.04	0.12	NNN	LCC
62179	64	21.14	1.40	1.02	0.04	1.00	0.04	0.93	0.07	NNN	LCC
62205	20	8.80	0.72	1.01	0.03	0.95	0.03	0.86	0.07	NNN	LCC
62226	38	2.53	0.84	1.00	0.03	1.03	0.04	1.69	0.56	NNN	LCC
62327	84	84.85	4.77	1.32	0.08	0.97	0.05	1.17	0.09	NNN	LCC
62427	65	12.12	0.95	0.99	0.03	1.03	0.03	2.41	0.20	NNY	LCC
62428	81	33.97	1.88	1.04	0.04	1.04	0.04	1.34	0.09	NNN	LCC
62431	59	11.83	1.23	1.00	0.03	0.98	0.03	0.84	0.09	NNN	LCC
62482	23	75.07	2.28	0.99	0.03	1.13	0.04	6.61	0.28	NNY	LCC
62488	34	16.65	0.94	1.00	0.03	1.09	0.03	2.12	0.13	NNY	LCC
62657	83	45.36	1.59	1.01	0.03	1.08	0.03	6.27	0.26	NNY	LCC
62683	62	88.68	2.12	1.39	0.09	0.87	0.05	0.86	0.05	NNN	LCC
62711	7	8.25	0.82	1.00	0.03	1.00	0.03	1.05	0.11	NNN	LCC
62723	22	4.00	0.87	0.98	0.03	0.98	0.03	1.14	0.25	NNN	LCC
62765	6	6.71	0.96	1.01	0.03	1.00	0.03	1.18	0.17	NNN	LCC
62786	55	29.10	1.29	0.96	0.04	0.91	0.04	1.08	0.06	NNN	LCC
62916	15	12.57	0.78	1.00	0.03	0.99	0.03	0.92	0.06	NNN	LCC
62941	13	4.24	0.87	1.00	0.03	1.02	0.03	0.99	0.20	NNN	LCC
63003	68	116.48	3.11	1.70	0.11	0.98	0.06	1.02	0.06	NNN	LCC
63005	81	355.66	6.88	1.51	0.10	2.07	0.12	5.57	0.33	YYY	LCC
63007	83	72.22	1.80	1.39	0.08	0.90	0.05	0.88	0.05	NNN	LCC
63022	27	2.38	0.75	1.00	0.03	0.98	0.03	0.93	0.30	NNN	LCC
63036	6	11.19	3.79	0.92	0.03	0.95	0.05	1.19	0.40	NNN	LCC
63085	9	18.58	0.99	0.99	0.04	0.98	0.03	1.02	0.06	NNN	LCC
63204	87	32.77	1.12	0.93	0.04	0.91	0.04	0.92	0.05	NNN	LCC
63210	75	62.21	1.66	1.20	0.07	0.93	0.05	1.01	0.06	NNN	LCC
63236	40	57.10	1.74	1.01	0.04	1.31	0.04	3.17	0.13	NNY	LCC
63246	43	8.19	0.93	1.00	0.03	1.00	0.03	1.18	0.14	NNN	LCC
63272	84	9.15	0.92	1.00	0.03	1.00	0.03	0.98	0.10	NNN	LCC
63395	22	6.59	0.90	0.99	0.03	1.07	0.04	1.68	0.23	NNY	LCC
63435	48	6.36	0.84	0.98	0.03	1.00	0.03	1.11	0.15	NNN	LCC
63439	70	12.06	0.98	1.00	0.03	1.08	0.03	2.29	0.19	NNY	LCC
63527	32	14.30	0.99	1.03	0.04	1.01	0.04	0.95	0.07	NNN	LCC
63540	10	4.53	0.95	0.99	0.03	0.99	0.03	1.26	0.27	NNN	LCC
63606	40	7.71	0.83	0.96	0.02	0.96	0.02	1.05	0.11	NNN	LCC
63678	8	25.18	1.11	0.99	0.03	1.32	0.04	5.71	0.28	YYY	LCC
63819	6	6.58	0.87	0.99	0.03	1.02	0.03	1.33	0.18	NNN	LCC
63836	85	9.77	0.88	1.00	0.03	1.04	0.03	1.53	0.14	NNY	LCC
63839	73	94.68	2.79	1.02	0.04	1.53	0.05	5.27	0.22	NNY	LCC
63886	75	21.35	1.04	1.00	0.03	1.03	0.03	1.90	0.10	NNY	LCC
63935	9	8.54	0.77	1.02	0.03	1.01	0.03	1.07	0.10	NNN	LCC
63975	57	1600.44	16.21	1.32	0.06	13.28	0.53	64.29	2.40	YYY	LCC
64004	73	86.43	2.23	1.30	0.08	0.87	0.05	0.88	0.05	NNN	LCC
64033	27	242.01	4.68	1.47	0.10	0.90	0.06	0.87	0.05	NNN	LCC
64044	78	10.16	1.01	0.99	0.03	0.98	0.03	1.12	0.11	NNN	LCC
64053	82	81.78	1.96	1.10	0.05	1.14	0.05	2.01	0.10	NNY	LCC
64184	81	219.30	4.44	1.00	0.03	1.25	0.04	18.44	0.60	NNY	LCC
64204	10	13.66	1.21	0.96	0.04	0.95	0.04	0.98	0.09	NNN	LCC
64264	58	9.40	1.17	0.98	0.03	0.96	0.03	0.80	0.10	NNN	LCC

Table 4: The WISE band 4 flux and  $W_2, W_3$  and  $W_4$  flux as a multiple of the photosphere with errors for our sample. <sup>a</sup> This column indicates the detection of an excess in the three colours. The lower section of the table displays the objects removed from our sample due to poor photometry or unreliable images.

HIP	P	$F_{W_4}$ (mJy)	$\sigma_{F_{W_4}}$ (mJy)	$R(W_2)$	$\sigma_{R(W_2)}$	$R(W_3)$	$\sigma_{R(W_3)}$	$R(W_4)$	$\sigma_{R(W_4)}$	Excess <sup>a</sup>	Subgroup
64316	42	2.13	0.82	0.98	0.03	0.95	0.03	0.91	0.35	NNN	LCC
64320	70	26.88	1.11	0.99	0.04	0.94	0.04	1.00	0.06	NNN	LCC
64322	74	21.63	4.32	0.99	0.03	1.04	0.04	1.76	0.36	NNY	LCC
64372	30	7.85	0.78	0.98	0.03	0.94	0.03	0.78	0.08	NNN	LCC
64425	54	111.65	2.67	1.39	0.08	0.97	0.05	1.06	0.06	NNN	LCC
64515	71	33.04	1.40	1.04	0.05	0.96	0.04	0.94	0.05	NNN	LCC
64560	21	2.98	0.83	1.01	0.03	1.03	0.03	1.10	0.31	NNN	LCC
64565	16	19.07	0.91	1.01	0.04	0.95	0.03	0.91	0.05	NNN	LCC
64570	35	6.43	1.09	0.99	0.03	0.97	0.03	0.84	0.14	NNN	LCC
64617	51	12.42	1.03	1.00	0.03	0.98	0.03	0.99	0.09	NNN	LCC
64661	47	75.34	1.94	1.48	0.08	1.01	0.05	0.97	0.05	NNN	LCC
64752	32	7.91	0.87	0.99	0.03	0.99	0.03	1.18	0.13	NNN	LCC
64837	69	23.43	1.17	1.00	0.03	1.12	0.03	1.98	0.11	NNY	LCC
64846	28	3.30	0.92	0.98	0.03	0.98	0.03	0.82	0.23	NNN	LCC
64892	74	16.33	1.02	1.00	0.03	0.99	0.03	1.10	0.08	NNN	LCC
64925	80	13.94	1.04	1.02	0.03	1.01	0.03	1.00	0.08	NNN	LCC
64933	8	30.86	1.14	1.03	0.05	0.99	0.04	1.01	0.05	NNN	LCC
64975	11	3.02	0.88	1.01	0.03	1.02	0.04	1.43	0.42	NNN	LCC
64995	79	118.32	2.40	0.94	0.03	1.05	0.03	10.64	0.32	NNY	LCC
65021	59	9.24	0.86	0.98	0.03	0.99	0.03	0.91	0.09	NNN	LCC
65089	84	23.67	1.13	1.00	0.03	1.08	0.03	2.39	0.13	NNY	LCC
65136	63	4.42	0.85	1.04	0.03	1.05	0.03	1.15	0.22	NNN	LCC
65178	61	17.91	1.11	0.98	0.03	0.98	0.03	1.07	0.07	NNN	LCC
65215	11	3.86	0.78	0.99	0.03	0.98	0.03	0.80	0.16	NNN	LCC
65271	62	99.69	3.95	1.55	0.09	0.91	0.05	1.08	0.07	NNN	LCC
65348	50	5.31	0.91	1.00	0.03	1.00	0.03	1.04	0.18	NNN	LCC
65394	67	9.71	0.88	0.99	0.03	1.00	0.03	0.95	0.09	NNN	LCC
65426	76	17.45	0.95	0.96	0.03	0.99	0.03	1.05	0.07	NNN	LCC
65502	7	9.85	0.92	1.02	0.03	1.00	0.03	0.99	0.09	NNN	LCC
65504	16	8.98	0.98	0.99	0.03	0.97	0.03	1.14	0.13	NNN	UCL
65517	69	5.47	0.87	0.99	0.03	0.98	0.03	0.98	0.16	NNN	LCC
65529	7	5.19	0.96	0.99	0.03	0.98	0.03	0.75	0.14	NNN	UCL
65546	7	8.75	1.16	0.98	0.03	0.98	0.03	0.95	0.13	NNN	UCL
65617	64	4.01	0.70	0.99	0.03	1.01	0.04	0.96	0.17	NNN	LCC
65875	88	203.16	4.12	0.99	0.04	1.17	0.04	12.81	0.46	NNY	LCC
65910	15	7.54	1.01	0.98	0.03	1.00	0.03	0.94	0.13	NNN	LCC
65965	70	43.00	1.47	1.00	0.03	1.30	0.04	5.38	0.22	NNY	LCC
66063	11	9.01	0.99	1.00	0.03	0.99	0.03	1.13	0.13	NNN	UCL
66068	75	50.47	1.63	0.98	0.03	1.28	0.04	4.04	0.17	NNY	LCC
66075	56	25.41	0.98	0.99	0.03	1.01	0.03	2.06	0.10	NNY	LCC
66152	49	23.01	1.12	1.07	0.04	1.07	0.04	1.01	0.06	NNN	LCC
66160	34	3.76	1.08	0.99	0.03	1.01	0.03	0.96	0.28	NNN	UCL
66255	29	8.80	0.88	0.99	0.03	0.99	0.03	1.16	0.12	NNN	LCC
66454	89	27.15	1.20	1.05	0.04	1.01	0.04	1.01	0.06	NNN	LCC
66566	82	44.90	1.49	1.00	0.03	1.28	0.04	4.80	0.20	NNY	LCC
66642	16	6.03	0.67	0.98	0.03	0.94	0.03	0.81	0.09	NNN	LCC
66651	75	9.80	0.84	1.04	0.03	1.06	0.03	1.11	0.10	NNN	LCC
66701	12	3.15	0.75	0.99	0.03	0.97	0.03	0.65	0.16	NNN	LCC
66722	92	25.96	1.05	1.07	0.04	1.05	0.04	1.14	0.06	NNN	UCL
66764	8	6.80	1.05	0.99	0.03	0.97	0.03	0.96	0.15	NNN	UCL
66884	12	4.63	0.96	0.99	0.03	1.00	0.03	1.24	0.26	NNN	UCL
66908	88	14.49	0.89	0.99	0.04	0.98	0.04	0.93	0.06	NNN	UCL
67036	81	14.54	1.03	0.97	0.04	0.96	0.03	0.88	0.07	NNN	LCC
67068	80	10.92	0.86	1.01	0.03	1.02	0.03	1.21	0.10	NNN	LCC
67075	49	9.71	0.99	0.99	0.03	0.99	0.03	1.00	0.11	NNN	UCL
67114	13	3.11	1.04	1.00	0.03	0.99	0.03	1.13	0.38	NNN	UCL

Table 4: The WISE band 4 flux and  $W_2, W_3$  and  $W_4$  flux as a multiple of the photosphere with errors for our sample. <sup>a</sup> This column indicates the detection of an excess in the three colours. The lower section of the table displays the objects removed from our sample due to poor photometry or unreliable images.

HIP	P	$F_{W_4}$ (mJy)	$\sigma_{F_{W_4}}$ (mJy)	R( $W_2$ )	$\sigma_{R(W_2)}$	R( $W_3$ )	$\sigma_{R(W_3)}$	R( $W_4$ )	$\sigma_{R(W_4)}$	Excess <sup>a</sup>	Subgroup
67230	65	37.07	3.59	1.02	0.04	1.05	0.05	2.46	0.25	NNY	LCC
67260	61	15.54	1.02	0.99	0.03	0.98	0.03	0.90	0.06	NNN	LCC
67277	20	13.36	1.14	0.96	0.03	0.93	0.03	0.87	0.08	NNN	UCL
67306	33	12.87	0.90	1.00	0.03	0.99	0.03	0.99	0.08	NNN	UCL
67334	46	7.81	0.91	1.00	0.03	1.01	0.03	1.10	0.13	NNN	UCL
67360	6	2.17	0.83	0.98	0.03	0.95	0.03	0.54	0.21	NNN	LCC
67407	7	6.30	1.14	0.98	0.03	0.94	0.03	0.79	0.14	NNN	UCL
67428	73	13.80	0.93	1.00	0.03	1.02	0.03	1.70	0.12	NNY	LCC
67440	6	4.54	0.99	0.98	0.03	0.97	0.03	1.19	0.26	NNN	UCL
67441	8	7.02	0.98	1.05	0.03	1.04	0.03	0.98	0.14	NNN	LCC
67448	25	7.65	1.04	0.99	0.03	0.98	0.03	0.84	0.12	NNN	UCL
67464	57	170.23	5.02	1.72	0.13	0.94	0.06	0.95	0.07	NNN	UCL
67472	54	560.07	10.83	1.77	0.12	1.58	0.10	3.31	0.21	NYY	UCL
67477	13	2.39	1.05	1.00	0.03	1.03	0.04	0.87	0.38	NNN	UCL
67497	92	89.75	2.48	1.00	0.03	1.16	0.04	10.42	0.39	NNY	UCL
67669	66	220.72	4.68	1.38	0.09	1.62	0.10	3.27	0.21	YYY	UCL
67844	17	15.24	2.06	1.00	0.03	1.00	0.04	1.28	0.18	NNN	LCC
67859	30	13.21	1.06	1.04	0.04	0.99	0.03	1.02	0.09	NNN	UCL
67916	7	9.02	0.86	1.00	0.03	1.01	0.03	1.11	0.11	NNN	LCC
67919	66	23.74	1.01	1.01	0.04	0.99	0.04	1.06	0.06	NNN	LCC
67957	89	7.51	0.96	1.03	0.06	0.98	0.06	0.90	0.12	NNN	UCL
67970	90	29.47	1.33	1.00	0.03	1.15	0.03	3.94	0.20	NNY	UCL
68245	76	116.91	2.58	1.80	0.12	0.96	0.06	0.92	0.06	YNN	UCL
68282	77	113.93	2.73	1.58	0.10	0.91	0.05	0.88	0.05	NNN	UCL
68335	87	11.33	0.90	1.00	0.03	1.00	0.03	0.98	0.08	NNN	UCL
68454	7	7.67	0.73	1.00	0.03	1.00	0.03	0.95	0.09	NNN	UCL
68722	72	6.62	1.13	1.00	0.03	0.99	0.03	0.93	0.16	NNN	UCL
68781	89	17.24	0.97	1.00	0.03	1.12	0.03	1.83	0.11	NNY	UCL
68854	7	8.01	1.10	0.99	0.03	0.99	0.03	1.21	0.17	NNN	UCL
68862	58	74.79	2.00	1.34	0.07	0.92	0.04	0.91	0.05	NNN	UCL
68867	56	11.45	1.16	0.99	0.03	0.99	0.03	1.01	0.11	NNN	UCL
68958	42	19.40	0.89	1.01	0.04	1.00	0.04	1.15	0.06	NNN	UCL
69011	77	149.36	2.89	1.01	0.04	1.23	0.05	6.89	0.27	NYY	UCL
69113	80	26.56	1.32	0.95	0.04	0.91	0.04	0.97	0.06	NNN	UCL
69291	88	8.75	1.01	1.00	0.03	0.99	0.03	1.17	0.14	NNN	UCL
69300	23	13.31	0.90	0.99	0.03	1.05	0.04	1.14	0.08	NNN	UCL
69302	82	7.76	0.79	0.99	0.03	1.00	0.03	1.05	0.11	NNN	UCL
69327	45	8.65	0.88	1.00	0.03	1.00	0.03	1.20	0.13	NNN	UCL
69475	59	12.89	1.03	0.99	0.03	0.98	0.03	0.94	0.08	NNN	UCL
69605	26	6.80	1.04	0.99	0.03	1.02	0.03	1.19	0.18	NNN	UCL
69618	71	775.25	11.42	2.47	0.15	3.30	0.17	7.48	0.38	NYY	UCL
69659	31	6.76	0.92	1.00	0.03	1.00	0.03	1.14	0.16	NNN	UCL
69693	12	1.62	0.78	0.99	0.03	1.03	0.05	1.61	0.77	NNN	UCL
69720	83	9.71	0.91	1.00	0.03	1.07	0.03	1.51	0.15	NNY	UCL
69791	60	6.23	0.79	1.00	0.03	1.00	0.03	1.22	0.16	NNN	UCL
69897	7	6.74	0.67	0.99	0.03	1.01	0.03	1.25	0.13	NNN	UCL
69990	21	6.57	0.91	0.99	0.03	1.00	0.03	1.13	0.16	NNN	UCL
69995	70	61.02	2.53	1.12	0.05	1.14	0.05	1.40	0.08	NNY	UCL
70050	37	15.74	1.32	1.00	0.03	1.02	0.03	1.18	0.10	NNN	UCL
70149	90	13.53	1.00	0.99	0.03	1.10	0.03	2.72	0.21	NNY	UCL
70300	86	76.18	2.10	1.46	0.08	0.94	0.05	0.93	0.05	YNN	UCL
70350	70	20.50	1.11	1.05	0.04	1.01	0.03	1.12	0.07	NNN	UCL
70441	93	25.37	1.07	0.99	0.03	1.10	0.03	2.58	0.13	NNY	UCL
70455	51	27.51	1.09	1.01	0.04	1.16	0.04	2.39	0.12	NNY	UCL
70483	52	27.43	1.09	1.08	0.04	1.02	0.04	1.04	0.05	NNN	UCL
70513	20	18.84	1.09	1.03	0.04	0.99	0.04	1.02	0.07	NNN	UCL

Table 4: The WISE band 4 flux and  $W_2, W_3$  and  $W_4$  flux as a multiple of the photosphere with errors for our sample. <sup>a</sup> This column indicates the detection of an excess in the three colours. The lower section of the table displays the objects removed from our sample due to poor photometry or unreliable images.

HIP	P	$F_{W_4}$ (mJy)	$\sigma_{F_{W_4}}$ (mJy)	$R(W_2)$	$\sigma_{R(W_2)}$	$R(W_3)$	$\sigma_{R(W_3)}$	$R(W_4)$	$\sigma_{R(W_4)}$	Excess <sup>a</sup>	Subgroup
70537	28	8.59	0.94	0.99	0.03	0.99	0.03	1.08	0.12	NNN	UCL
70558	88	3.99	0.87	1.01	0.03	1.01	0.03	0.82	0.18	NNN	UCL
70575	7	2.14	0.79	1.00	0.03	0.99	0.03	0.72	0.26	NNN	LCC
70626	79	19.85	0.93	1.00	0.04	0.97	0.04	1.06	0.06	NNN	UCL
70676	16	2.56	0.77	0.98	0.03	0.97	0.03	0.91	0.27	NNN	UCL
70689	90	8.23	0.83	1.02	0.03	0.99	0.03	0.93	0.10	NNN	UCL
70697	89	11.20	0.80	1.00	0.03	0.99	0.03	1.01	0.08	NNN	UCL
70753	80	67.15	1.73	1.25	0.08	0.92	0.05	0.89	0.05	NNN	UCL
70809	68	20.79	1.23	1.00	0.04	0.99	0.04	1.10	0.07	NNN	UCL
70822	27	5.31	0.90	0.99	0.03	1.00	0.03	0.93	0.16	NNN	UCL
70833	84	5.33	0.90	0.99	0.03	0.99	0.03	0.77	0.13	NNN	UCL
70898	28	9.97	1.06	1.02	0.03	1.00	0.03	1.05	0.11	NNN	UCL
70904	66	23.03	1.08	1.05	0.04	1.00	0.04	0.97	0.06	NNN	UCL
70977	5	3.19	0.88	0.98	0.03	1.02	0.03	1.01	0.28	NNN	UCL
70998	89	12.56	1.11	1.01	0.03	0.99	0.03	0.97	0.09	NNN	UCL
71023	32	6.63	0.85	0.99	0.03	1.01	0.03	1.20	0.16	NNN	UCL
71140	67	11.60	0.97	0.98	0.03	0.98	0.03	0.95	0.08	NNN	UCL
71271	55	19.91	1.06	1.00	0.03	1.12	0.03	2.52	0.15	NNY	UCL
71314	7	9.55	0.86	0.99	0.03	0.96	0.03	0.84	0.08	NNN	LCC
71321	92	11.97	1.00	1.04	0.03	1.02	0.03	1.03	0.09	NNN	UCL
71352	82	2256.53	29.10	1.83	0.10	2.26	0.13	3.99	0.22	NNY	UCL
71453	66	37.62	1.28	1.03	0.04	0.98	0.04	1.19	0.06	NNN	UCL
71498	41	5.14	0.79	1.01	0.03	1.02	0.03	1.15	0.18	NNN	UCL
71536	84	119.85	3.09	1.67	0.11	0.97	0.06	0.95	0.06	NNN	UCL
71633	36	8.19	0.96	1.00	0.03	0.98	0.03	0.90	0.11	NNN	UCL
71708	84	8.92	0.88	0.99	0.03	1.03	0.03	1.28	0.13	NNN	UCL
71724	83	16.11	1.10	0.94	0.03	0.94	0.03	0.93	0.07	NNN	UCL
71767	43	8.12	0.96	1.02	0.03	1.02	0.03	1.14	0.14	NNN	UCL
71835	14	7.60	0.99	1.01	0.03	1.03	0.03	1.08	0.14	NNN	UCL
71858	15	2.44	1.09	0.98	0.03	0.90	0.03	0.53	0.24	NNN	UCL
71865	93	113.72	3.14	1.58	0.11	0.95	0.06	0.94	0.06	NNN	UCL
71885	9	5.81	0.93	0.99	0.03	1.02	0.04	1.56	0.25	NNY	UCL
71969	13	6.32	0.97	0.98	0.03	0.97	0.03	0.94	0.15	NNN	US
71982	33	12.60	1.19	0.99	0.03	0.98	0.03	1.09	0.11	NNN	UCL
72060	16	18.91	1.20	0.99	0.03	0.95	0.03	0.95	0.07	NNN	US
72099	47	11.46	1.08	1.00	0.03	1.14	0.03	2.90	0.28	NNY	UCL
72140	22	10.81	0.94	0.99	0.03	0.96	0.03	0.85	0.08	NNN	UCL
72149	51	4.81	1.00	1.01	0.03	1.01	0.03	1.58	0.33	NNN	UCL
72158	59	12.10	1.04	1.01	0.03	0.98	0.03	1.04	0.09	NNN	UCL
72164	28	5.38	1.04	0.99	0.03	0.98	0.03	0.98	0.19	NNN	UCL
72185	12	4.06	0.85	0.99	0.03	0.99	0.03	0.85	0.18	NNN	UCL
72299	27	11.58	1.17	1.00	0.03	0.98	0.03	1.20	0.13	NNN	UCL
72345	18	3.31	1.09	1.00	0.03	0.99	0.03	0.90	0.30	NNN	UCL
72352	22	5.16	0.84	0.99	0.03	1.01	0.03	1.10	0.18	NNN	UCL
72411	30	12.02	1.03	0.98	0.03	0.95	0.03	0.98	0.09	NNN	UCL
72584	78	13.93	0.97	0.99	0.03	1.04	0.03	1.79	0.13	NNY	UCL
72627	93	21.08	1.20	1.02	0.04	1.00	0.04	1.00	0.07	NNN	UCL
72630	41	2.75	0.95	0.99	0.03	0.98	0.03	0.73	0.25	NNN	UCL
72683	74	90.92	2.26	1.54	0.10	0.92	0.05	0.89	0.06	NNN	UCL
72771	13	7.49	1.07	0.98	0.03	0.96	0.03	0.87	0.13	NNN	US
72800	71	46.89	1.47	1.18	0.07	0.95	0.05	0.88	0.05	NNN	UCL
72877	6	2.57	0.83	1.01	0.03	1.05	0.04	1.33	0.43	NNN	UCL
72904	12	4.84	0.81	1.01	0.03	1.00	0.03	1.07	0.18	NNN	UCL
72938	26	5.63	0.94	0.99	0.03	1.03	0.03	1.46	0.25	NNN	UCL
72940	91	21.33	1.08	0.91	0.04	0.89	0.04	0.92	0.06	NNN	UCL
73145	91	156.98	3.18	1.02	0.03	1.82	0.05	19.72	0.63	NNY	UCL

Table 4: The WISE band 4 flux and  $W_2, W_3$  and  $W_4$  flux as a multiple of the photosphere with errors for our sample. <sup>a</sup> This column indicates the detection of an excess in the three colours. The lower section of the table displays the objects removed from our sample due to poor photometry or unreliable images.

HIP	P	$F_{W_4}$ (mJy)	$\sigma_{F_{W_4}}$ (mJy)	R( $W_2$ )	$\sigma_{R(W_2)}$	R( $W_3$ )	$\sigma_{R(W_3)}$	R( $W_4$ )	$\sigma_{R(W_4)}$	Excess <sup>a</sup>	Subgroup
73147	78	6.27	0.93	0.98	0.03	1.02	0.03	1.13	0.17	NNN	UCL
73171	33	33.32	1.35	0.99	0.04	0.98	0.04	1.24	0.07	NNN	UCL
73266	92	10.27	1.04	0.99	0.03	1.00	0.03	1.05	0.11	NNN	UCL
73274	8	2.64	0.86	0.99	0.03	0.98	0.03	0.76	0.25	NNN	US
73295	13	10.98	0.98	1.02	0.03	1.02	0.03	1.10	0.10	NNN	UCL
73334	73	236.94	4.80	1.92	0.13	0.89	0.06	0.89	0.06	NNN	UCL
73341	65	35.86	1.35	0.97	0.04	1.10	0.04	2.04	0.10	NNY	UCL
73348	7	13.20	0.79	1.00	0.03	0.99	0.03	1.03	0.07	NNN	UCL
73357	32	21.47	1.46	1.03	0.04	0.97	0.03	1.01	0.08	NNN	UCL
73358	12	13.91	1.20	1.01	0.04	0.96	0.03	0.94	0.09	NNN	US
73393	21	11.55	0.87	0.99	0.03	0.99	0.03	1.10	0.09	NNN	UCL
73409	19	11.65	1.38	1.01	0.03	0.99	0.03	0.91	0.11	NNN	UCL
73498	10	2.65	0.93	1.00	0.03	0.98	0.03	0.67	0.24	NNN	US
73535	62	12.28	0.97	0.97	0.03	0.95	0.03	0.92	0.08	NNN	UCL
73538	21	3.24	0.90	0.98	0.03	0.96	0.03	0.87	0.24	NNN	UCL
73559	61	50.10	1.52	1.20	0.06	0.96	0.05	0.96	0.05	YNN	UCL
73597	15	4.52	0.84	0.99	0.03	1.01	0.03	1.21	0.23	NNN	UCL
73624	86	36.77	1.39	1.12	0.05	0.95	0.04	0.94	0.05	NNN	UCL
73667	36	6.65	0.92	0.99	0.03	0.98	0.03	0.90	0.13	NNN	UCL
73698	5	7.54	1.01	1.01	0.03	1.00	0.03	0.90	0.12	NNN	UCL
73742	58	10.61	0.94	0.97	0.03	0.95	0.03	0.89	0.08	NNN	UCL
73766	46	16.18	1.10	1.02	0.04	0.99	0.03	1.01	0.07	NNN	US
73807	76	138.50	3.06	1.59	0.11	0.95	0.06	0.91	0.06	NNN	UCL
73828	10	6.03	0.99	0.99	0.03	0.96	0.03	0.91	0.15	NNN	UCL
73859	11	7.44	1.31	1.00	0.03	0.94	0.03	1.05	0.19	NNN	US
73906	16	8.33	2.50	1.00	0.03	0.97	0.03	1.21	0.36	NNN	US
73913	88	7.42	0.94	1.02	0.03	1.03	0.03	1.11	0.14	NNN	UCL
73990	81	44.04	1.58	1.02	0.03	1.25	0.04	4.39	0.19	YY	UCL
74066	67	33.65	1.49	1.00	0.04	0.91	0.04	0.97	0.06	NNN	UCL
74098	67	6.68	1.24	1.00	0.03	0.94	0.03	1.10	0.20	NNN	UCL
74100	87	29.45	1.19	1.05	0.04	1.01	0.04	1.05	0.06	NNN	UCL
74104	74	7.93	0.86	1.01	0.03	1.00	0.03	1.04	0.12	NNN	UCL
74114	49	3.33	1.01	1.00	0.03	0.98	0.03	0.47	0.14	NNN	UCL
74125	10	8.11	1.18	1.00	0.03	0.96	0.03	0.98	0.15	NNN	US
74181	6	30.16	1.28	1.04	0.05	0.95	0.04	0.90	0.05	NNN	UCL
74308	47	5.32	0.93	0.96	0.03	0.93	0.03	0.71	0.12	NNN	UCL
74449	48	55.19	1.68	1.18	0.06	0.91	0.05	0.89	0.05	NNN	UCL
74468	70	8.78	1.52	0.98	0.04	1.05	0.04	1.31	0.23	NNN	UCL
74479	78	23.39	1.18	0.99	0.04	0.93	0.04	0.91	0.06	NNN	UCL
74490	39	21.81	1.25	0.98	0.04	0.95	0.04	0.99	0.06	NNN	UCL
74498	44	5.98	0.92	1.00	0.03	0.98	0.03	1.51	0.23	NNN	UCL
74499	90	23.85	1.19	0.99	0.03	1.04	0.03	3.10	0.17	YY	UCL
74529	43	7.04	1.22	1.07	0.03	1.05	0.03	1.10	0.19	NNN	UCL
74645	20	7.11	0.77	1.00	0.03	0.97	0.03	0.86	0.10	NNN	US
74651	62	8.06	1.03	1.00	0.03	0.98	0.03	1.13	0.15	NNN	UCL
74657	21	12.23	1.13	0.98	0.03	0.99	0.03	0.92	0.09	NNN	UCL
74724	7	8.68	0.81	0.98	0.03	0.96	0.03	0.91	0.09	NNN	UCL
74744	5	3.96	0.69	0.99	0.03	1.00	0.03	0.95	0.17	NNN	UCL
74752	21	19.65	1.09	0.99	0.03	1.07	0.04	1.28	0.08	NNN	UCL
74772	16	2.37	0.85	1.00	0.03	1.04	0.03	0.80	0.29	NNN	UCL
74820	5	5.83	1.07	0.97	0.03	0.88	0.03	1.23	0.23	NNN	UCL
74865	90	6.41	1.22	0.99	0.03	0.98	0.03	0.97	0.19	NNN	UCL
74911	62	396.86	8.77	1.93	0.12	1.60	0.09	2.84	0.16	YY	UCL
74959	84	8.15	0.95	0.98	0.03	0.99	0.03	1.65	0.20	NNY	UCL
74985	81	9.76	1.05	0.99	0.03	1.03	0.03	1.17	0.13	NNN	UCL
74992	34	11.02	1.07	1.01	0.03	1.04	0.03	1.14	0.11	NNN	US

Table 4: The WISE band 4 flux and  $W_2, W_3$  and  $W_4$  flux as a multiple of the photosphere with errors for our sample. <sup>a</sup> This column indicates the detection of an excess in the three colours. The lower section of the table displays the objects removed from our sample due to poor photometry or unreliable images.

HIP	P	$F_{W_4}$ (mJy)	$\sigma_{F_{W_4}}$ (mJy)	$R(W_2)$	$\sigma_{R(W_2)}$	$R(W_3)$	$\sigma_{R(W_3)}$	$R(W_4)$	$\sigma_{R(W_4)}$	Excess <sup>a</sup>	Subgroup
75035	61	8.24	0.98	1.03	0.03	0.97	0.03	0.90	0.11	NNN	UCL
75056	84	8.48	0.94	1.00	0.03	0.98	0.03	0.79	0.09	NNN	UCL
75077	78	17.68	1.11	0.97	0.04	1.00	0.04	1.26	0.09	NNN	UCL
75164	78	39.87	1.54	1.04	0.05	1.00	0.04	1.19	0.07	NNN	UCL
75210	91	46.84	1.51	0.98	0.04	1.20	0.04	2.93	0.13	NYY	UCL
75264	47	189.78	3.67	1.57	0.12	0.92	0.06	0.89	0.06	NNN	UCL
75267	18	4.76	0.87	0.99	0.03	0.98	0.03	1.06	0.20	NNN	UCL
75290	30	5.38	0.90	1.00	0.03	0.98	0.03	0.78	0.13	NNN	UCL
75304	90	74.86	2.21	1.48	0.09	1.07	0.06	1.05	0.06	YNN	UCL
75367	80	3.12	0.84	1.00	0.03	1.01	0.03	1.15	0.31	NNN	UCL
75403	6	2.92	0.95	1.02	0.03	1.03	0.04	1.10	0.36	NNN	UCL
75427	23	9.99	0.89	0.98	0.03	0.98	0.03	0.97	0.09	NNN	UCL
75459	41	9.30	0.89	0.99	0.03	0.97	0.03	1.01	0.10	NNN	UCL
75476	82	17.39	1.09	1.03	0.04	1.05	0.04	1.17	0.08	NNN	UCL
75480	89	9.39	1.08	1.00	0.03	0.98	0.03	0.96	0.11	NNN	UCL
75491	70	27.05	1.30	0.97	0.03	1.01	0.03	2.81	0.15	NYY	UCL
75509	92	27.25	2.08	1.01	0.03	1.27	0.05	2.98	0.24	NYY	UCL
75575	12	5.47	0.90	1.02	0.03	1.00	0.03	0.83	0.14	NNN	UCL
75612	12	5.48	0.87	1.00	0.03	0.97	0.03	1.04	0.17	NNN	UCL
75613	52	14.92	0.98	0.99	0.04	0.94	0.03	0.94	0.07	NNN	UCL
75647	83	33.22	1.22	1.02	0.05	0.93	0.04	0.91	0.05	NNN	UCL
75659	40	3.39	1.02	0.98	0.03	0.96	0.03	0.75	0.23	NNN	US
75669	26	4.04	0.97	0.99	0.03	0.99	0.03	0.81	0.20	NNN	US
75683	83	8.09	1.09	1.01	0.03	1.06	0.03	2.01	0.27	NYY	UCL
75765	17	13.55	0.95	1.00	0.04	0.94	0.03	0.87	0.07	NNN	UCL
75802	50	7.67	1.02	0.99	0.03	0.95	0.03	0.89	0.12	NNN	UCL
75824	69	5.31	0.93	1.02	0.02	1.02	0.02	0.80	0.14	NNN	UCL
75891	90	7.83	0.95	1.00	0.03	1.00	0.03	0.94	0.12	NNN	UCL
75902	6	15.41	0.88	0.99	0.03	1.13	0.04	2.83	0.18	NYY	UCL
75906	9	4.70	1.00	0.98	0.03	0.95	0.03	0.69	0.15	NNN	US
75933	34	6.93	0.89	1.01	0.03	1.03	0.03	0.94	0.12	NNN	UCL
75935	28	5.15	1.02	1.00	0.03	0.99	0.03	0.82	0.16	NNN	US
75952	7	4.73	0.93	0.99	0.03	1.02	0.03	1.20	0.24	NNN	UCL
75957	26	11.94	1.02	1.01	0.03	1.00	0.03	1.11	0.10	NNN	UCL
75985	9	19.69	1.14	1.04	0.04	1.00	0.04	1.14	0.07	NNN	US
76001	73	21.89	1.31	1.02	0.04	0.98	0.04	0.97	0.07	NNN	UCL
76048	83	28.75	1.19	1.00	0.04	0.98	0.04	1.10	0.06	NNN	UCL
76071	70	11.67	1.15	0.99	0.03	0.94	0.03	0.90	0.09	NNN	US
76084	87	9.40	1.00	1.00	0.03	0.96	0.03	1.06	0.12	NNN	UCL
76223	47	74.17	2.39	0.99	0.03	1.21	0.04	5.71	0.24	NYY	UCL
76234	73	63.89	1.71	0.98	0.04	1.19	0.05	2.83	0.12	NYY	UCL
76264	14	6.45	1.02	1.01	0.03	1.02	0.03	0.91	0.14	NNN	UCL
76297	91	311.77	8.04	1.70	0.11	0.93	0.06	0.87	0.06	NNN	UCL
76302	36	6.32	1.04	1.00	0.03	0.99	0.03	1.12	0.19	NNN	US
76310	69	168.83	3.58	1.00	0.03	1.53	0.05	15.19	0.51	NYY	US
76395	78	67.71	2.06	1.03	0.04	1.49	0.05	3.26	0.14	NYY	UCL
76442	29	6.59	0.90	0.99	0.03	0.99	0.03	0.96	0.13	NNN	UCL
76501	50	9.18	0.97	1.00	0.03	0.99	0.03	0.97	0.10	NNN	UCL
76503	27	25.98	1.39	0.99	0.04	0.90	0.03	0.94	0.06	NNN	US
76549	47	16.03	1.98	0.96	0.04	0.92	0.04	0.83	0.11	NNN	UCL
76572	30	2.76	0.96	1.00	0.03	0.98	0.03	1.16	0.40	NNN	US
76591	64	14.83	1.01	1.01	0.04	1.01	0.04	0.94	0.07	NNN	UCL
76600	53	154.82	3.85	1.82	0.13	1.02	0.07	0.98	0.07	NNN	UCL
76633	89	8.14	1.03	0.99	0.03	1.04	0.03	0.99	0.13	NNN	US
76712	31	7.91	0.91	0.95	0.02	0.93	0.02	1.17	0.14	NNN	UCL
76782	39	63.71	2.29	0.97	0.03	1.00	0.04	4.43	0.21	NYY	US

Table 4: The WISE band 4 flux and  $W_2, W_3$  and  $W_4$  flux as a multiple of the photosphere with errors for our sample. <sup>a</sup> This column indicates the detection of an excess in the three colours. The lower section of the table displays the objects removed from our sample due to poor photometry or unreliable images.

HIP	P	$F_{W_4}$ (mJy)	$\sigma_{F_{W_4}}$ (mJy)	R( $W_2$ )	$\sigma_{R(W_2)}$	R( $W_3$ )	$\sigma_{R(W_3)}$	R( $W_4$ )	$\sigma_{R(W_4)}$	Excess <sup>a</sup>	Subgroup
76875	89	9.20	0.94	1.01	0.03	0.98	0.03	0.99	0.10	NNN	UCL
76887	11	3.93	1.01	0.99	0.03	0.99	0.03	0.83	0.21	NNN	US
76945	85	68.59	1.96	1.26	0.07	0.93	0.05	0.92	0.05	NNN	UCL
76997	62	9.83	1.01	0.99	0.03	0.98	0.03	1.03	0.11	NNN	UCL
77010	11	10.45	1.08	1.00	0.03	0.96	0.03	0.81	0.09	NNN	UCL
77038	88	6.53	0.97	1.00	0.03	1.00	0.03	1.08	0.16	NNN	UCL
77051	49	6.24	0.95	0.97	0.03	0.98	0.03	0.93	0.14	NNN	UCL
77124	56	4.64	1.13	0.98	0.03	0.97	0.03	0.82	0.20	NNN	US
77140	11	11.24	1.42	0.98	0.03	1.04	0.04	1.04	0.13	NNN	UCL
77144	79	6.86	0.89	1.00	0.03	0.98	0.03	1.07	0.14	NNN	UCL
77150	90	14.12	1.04	1.00	0.03	1.08	0.03	1.36	0.11	NNN	UCL
77154	34	3.47	1.00	1.03	0.03	0.99	0.03	1.22	0.35	NNN	US
77165	28	14.95	1.10	1.04	0.04	1.00	0.03	1.06	0.08	NNN	US
77286	84	35.11	1.36	1.07	0.05	0.96	0.04	1.01	0.06	NNN	UCL
77295	74	6.31	1.02	0.99	0.03	1.01	0.03	0.84	0.14	NNN	UCL
77315	45	63.66	2.05	1.03	0.04	1.25	0.05	3.66	0.16	NYY	UCL
77347	56	17.55	1.15	1.02	0.03	1.12	0.03	1.83	0.13	NNY	US
77378	19	2.28	0.99	1.01	0.03	0.99	0.04	1.17	0.51	NNN	UCL
77388	78	8.32	0.99	1.04	0.03	1.03	0.03	0.90	0.11	NNN	UCL
77398	9	3.03	1.13	0.99	0.03	0.94	0.03	0.76	0.28	NNN	UCL
77432	87	11.38	0.94	1.00	0.03	1.04	0.03	1.78	0.15	NNY	UCL
77502	62	6.67	1.00	1.00	0.03	0.99	0.03	1.04	0.16	NNN	UCL
77520	90	7.01	0.90	1.00	0.03	0.99	0.03	1.19	0.15	NNN	UCL
77523	33	18.77	1.24	0.98	0.03	1.12	0.04	2.09	0.15	NNY	UCL
77552	9	3.47	1.06	1.00	0.03	0.99	0.03	0.73	0.22	NNN	US
77588	43	5.09	1.05	0.99	0.03	0.96	0.03	0.85	0.18	NNN	US
77635	89	98.50	4.17	1.39	0.09	0.93	0.05	1.01	0.07	NNN	US
77713	45	4.81	1.04	0.99	0.03	0.98	0.03	0.95	0.21	NNN	UCL
77736	44	8.10	1.01	1.02	0.03	0.98	0.03	1.31	0.17	NNN	US
77766	6	7.36	1.10	1.01	0.03	1.01	0.03	0.96	0.15	NNN	US
77778	13	4.17	1.16	0.96	0.03	0.93	0.04	1.18	0.33	NNN	UCL
77815	79	11.94	1.08	1.02	0.03	1.01	0.03	0.99	0.09	NNN	US
77859	75	132.39	3.17	1.37	0.09	1.46	0.08	2.26	0.13	NYY	US
77900	82	21.51	1.23	1.03	0.04	0.98	0.04	0.93	0.06	NNN	US
77909	71	31.96	1.50	0.98	0.05	0.90	0.04	0.96	0.06	NNN	US
77937	17	5.10	0.85	1.03	0.03	0.99	0.03	0.83	0.14	NNN	UCL
77939	38	34.12	1.35	1.09	0.06	0.91	0.04	0.88	0.05	NNN	US
77960	86	9.99	1.08	1.00	0.03	0.98	0.03	1.00	0.11	NNN	US
77968	59	12.02	1.02	0.98	0.03	0.98	0.03	0.89	0.08	NNN	UCL
77974	5	8.66	1.00	0.98	0.03	0.98	0.03	0.91	0.11	NNN	UCL
78035	27	5.86	1.00	1.00	0.03	0.97	0.03	0.92	0.16	NNN	UCL
78043	83	12.83	1.00	0.99	0.03	1.06	0.03	2.19	0.18	NNY	UCL
78099	88	14.83	1.16	1.01	0.03	1.04	0.03	1.27	0.11	NNN	US
78104	82	117.01	3.13	1.55	0.09	0.99	0.05	0.96	0.06	NNN	US
78130	48	26.32	1.21	1.02	0.04	0.96	0.04	0.98	0.06	NNN	US
78150	84	11.12	1.93	1.00	0.03	0.98	0.04	0.98	0.17	NNN	UCL
78168	30	39.25	1.41	1.08	0.05	0.95	0.05	0.96	0.06	NNN	US
78183	88	17.68	1.17	0.97	0.04	0.91	0.03	1.00	0.07	NNN	US
78196	90	9.93	0.91	1.05	0.03	1.01	0.03	0.86	0.08	NNN	US
78197	5	9.18	0.92	0.98	0.03	0.97	0.03	1.01	0.10	NNN	UCL
78198	40	6.59	0.95	1.00	0.03	1.02	0.03	1.61	0.24	NNY	UCL
78207	86	839.92	20.89	2.23	0.14	2.58	0.14	5.15	0.29	NYY	US
78233	64	6.97	1.14	1.00	0.03	0.95	0.03	0.93	0.15	NNN	US
78246	23	40.28	1.48	1.02	0.05	0.93	0.04	0.92	0.05	NNN	US
78263	59	8.35	1.19	1.02	0.03	1.04	0.03	1.29	0.19	NNN	UCL
78264	37	12.07	0.98	0.97	0.03	0.93	0.03	1.01	0.09	NNN	UCL

Table 4: The WISE band 4 flux and  $W_2, W_3$  and  $W_4$  flux as a multiple of the photosphere with errors for our sample. <sup>a</sup> This column indicates the detection of an excess in the three colours. The lower section of the table displays the objects removed from our sample due to poor photometry or unreliable images.

HIP	P	$F_{W_4}$ (mJy)	$\sigma_{F_{W_4}}$ (mJy)	R( $W_2$ )	$\sigma_{R(W_2)}$	R( $W_3$ )	$\sigma_{R(W_3)}$	R( $W_4$ )	$\sigma_{R(W_4)}$	Excess <sup>a</sup>	Subgroup
78265	36	445.70	119.05	1.76	0.08	1.20	0.06	1.58	0.43	NNN	US
78266	10	4.13	1.39	1.00	0.03	0.97	0.05	1.23	0.42	NNN	UCL
78306	14	13.80	1.07	0.97	0.03	0.94	0.03	0.83	0.07	NNN	UCL
78324	78	9.92	1.01	1.01	0.03	1.00	0.03	1.14	0.12	NNN	UCL
78357	17	27.79	1.82	0.98	0.03	1.08	0.04	2.41	0.17	NNY	UCL
78381	27	4.85	0.98	1.00	0.03	0.98	0.03	1.04	0.21	NNN	US
78384	84	171.33	3.63	1.80	0.12	0.92	0.05	0.94	0.05	YNN	UCL
78494	54	14.72	1.49	1.02	0.03	0.96	0.04	0.99	0.10	NNN	US
78530	76	16.50	1.34	0.98	0.03	0.96	0.03	1.11	0.09	NNN	US
78533	88	18.07	1.13	1.07	0.03	1.05	0.03	1.45	0.10	NNY	UCL
78541	35	13.08	1.06	1.02	0.03	1.02	0.03	1.00	0.09	NNN	UCL
78549	89	15.73	1.29	1.03	0.04	1.00	0.04	1.17	0.10	NNN	US
78555	89	8.63	1.02	1.00	0.03	1.01	0.03	1.22	0.15	NNN	UCL
78573	6	5.22	1.06	1.01	0.03	0.96	0.03	0.70	0.14	NNN	US
78581	86	9.04	1.01	1.05	0.03	1.02	0.03	1.02	0.12	NNN	US
78603	32	27.43	1.16	1.02	0.04	1.04	0.04	1.13	0.06	NNN	UCL
78607	6	13.76	1.27	1.02	0.04	0.99	0.03	1.03	0.10	NNN	UCL
78611	12	12.37	1.00	0.97	0.03	0.97	0.03	1.22	0.10	NNN	UCL
78635	8	3.28	1.16	1.01	0.03	1.00	0.03	0.62	0.22	NNN	US
78641	91	52.61	1.89	0.98	0.03	1.31	0.04	6.79	0.29	NNY	UCL
78655	90	59.57	1.65	1.13	0.07	0.88	0.05	0.92	0.05	NNN	UCL
78663	88	8.80	1.09	0.98	0.03	0.99	0.03	1.19	0.15	NNN	US
78702	90	10.41	1.24	1.02	0.03	1.00	0.03	0.95	0.11	NNN	US
78711	63	4.53	0.98	0.99	0.03	0.93	0.03	0.79	0.17	NNN	UCL
78754	73	13.66	1.04	0.98	0.04	0.95	0.03	1.00	0.08	NNN	UCL
78766	12	6.53	0.91	1.00	0.03	1.01	0.03	1.19	0.17	NNN	UCL
78774	32	6.08	0.90	1.00	0.03	0.98	0.03	0.92	0.14	NNN	UCL
78795	37	7.65	0.95	0.97	0.03	0.95	0.03	0.91	0.12	NNN	UCL
78809	91	9.06	0.95	1.00	0.03	1.01	0.03	0.91	0.10	NNN	US
78826	44	12.60	1.02	1.02	0.03	1.02	0.03	1.42	0.12	NNY	UCL
78830	63	9.80	1.11	1.00	0.03	1.02	0.03	1.32	0.15	NNN	US
78847	89	11.63	0.97	1.02	0.04	0.99	0.03	0.95	0.08	NNN	US
78853	55	12.00	1.10	1.04	0.03	1.01	0.03	1.00	0.10	NNN	UCL
78877	61	44.90	2.11	0.97	0.05	0.88	0.04	1.13	0.07	NNN	US
78910	13	6.66	0.97	1.01	0.03	1.00	0.03	1.34	0.20	NNN	US
78918	72	98.68	2.27	1.51	0.09	0.93	0.05	0.96	0.05	NNN	UCL
78933	91	156.69	12.27	1.95	0.12	0.83	0.05	0.77	0.07	NNN	US
78943	49	7674.32	91.89	2.52	0.15	21.98	1.09	99.61	4.83	NNY	US
78956	93	17.28	1.16	0.99	0.03	1.04	0.03	1.51	0.11	NNY	US
78963	72	10.34	1.09	1.00	0.03	0.99	0.03	0.98	0.11	NNN	US
78968	89	15.84	1.11	0.98	0.03	1.07	0.03	1.67	0.12	NNY	US
78996	86	40.16	1.74	1.02	0.03	1.31	0.04	3.59	0.18	NNY	US
79044	81	14.15	0.98	0.97	0.03	0.98	0.03	1.02	0.08	NNN	UCL
79046	5	34.95	1.29	1.07	0.05	1.01	0.05	1.05	0.06	NNN	UCL
79054	91	9.20	1.25	1.00	0.03	1.07	0.04	1.38	0.19	NNN	US
79078	58	4.50	0.92	0.99	0.03	1.02	0.03	0.92	0.19	NNN	US
79081	63	34.41	12.87	0.99	0.04	1.05	0.09	1.83	0.69	NNN	UCL
79097	66	12.64	0.97	1.01	0.03	0.99	0.03	1.08	0.09	NNN	US
79124	82	15.93	1.12	1.02	0.04	1.00	0.03	1.15	0.09	NNN	US
79142	54	6.14	1.06	1.02	0.03	1.05	0.03	1.15	0.20	NNN	US
79156	88	23.78	1.20	1.01	0.03	1.28	0.04	2.57	0.14	NNY	US
79197	23	3.32	1.02	0.98	0.03	0.95	0.03	0.60	0.18	NNN	UCL
79235	23	27.63	1.32	1.07	0.04	1.01	0.04	1.04	0.06	NNN	US
79250	92	12.74	1.22	1.00	0.03	1.04	0.03	1.18	0.12	NNN	US
79288	87	447.75	8.25	1.18	0.03	12.11	0.36	68.39	2.02	YYY	US
79317	19	8.34	1.23	1.03	0.03	1.02	0.03	1.09	0.16	NNN	UCL

Table 4: The WISE band 4 flux and  $W_2, W_3$  and  $W_4$  flux as a multiple of the photosphere with errors for our sample. <sup>a</sup> This column indicates the detection of an excess in the three colours. The lower section of the table displays the objects removed from our sample due to poor photometry or unreliable images.

HIP	P	$F_{W_4}$ (mJy)	$\sigma_{F_{W_4}}$ (mJy)	R( $W_2$ )	$\sigma_{R(W_2)}$	R( $W_3$ )	$\sigma_{R(W_3)}$	R( $W_4$ )	$\sigma_{R(W_4)}$	Excess <sup>a</sup>	Subgroup
79366	87	11.50	1.11	1.00	0.03	0.96	0.03	1.04	0.10	NNN	US
79369	82	7.92	0.98	1.00	0.03	0.98	0.03	0.94	0.12	NNN	US
79372	33	23.35	1.05	1.03	0.04	1.00	0.04	1.04	0.06	NNN	UCL
79374	72	225.86	29.75	1.71	0.10	0.90	0.05	0.82	0.12	NNN	US
79383	74	15.28	1.00	1.00	0.03	1.13	0.03	2.44	0.17	NNY	US
79392	86	10.58	1.15	1.02	0.03	1.00	0.03	1.23	0.14	NNN	US
79410	79	42.60	1.61	1.02	0.03	1.36	0.04	3.37	0.15	NYY	US
79439	63	27.79	1.41	1.03	0.04	1.15	0.04	2.01	0.12	NNY	US
79454	28	4.14	0.99	1.00	0.03	0.98	0.03	1.14	0.27	NNN	US
79470	5	5.83	1.64	0.98	0.03	0.99	0.05	0.66	0.19	NNN	UCL
79478	19	16.12	1.13	1.04	0.03	1.07	0.03	1.30	0.10	NNN	UCL
79516	77	55.34	1.89	0.98	0.03	1.03	0.03	7.78	0.31	NNY	UCL
79530	79	28.62	1.34	1.03	0.04	0.91	0.04	0.89	0.05	NNN	US
79534	12	7.07	1.07	0.99	0.03	0.95	0.03	0.77	0.12	NNN	US
79552	35	11.94	1.08	1.02	0.03	0.99	0.03	0.84	0.08	NNN	US
79610	46	5.89	0.99	0.96	0.02	0.91	0.02	0.80	0.13	NNN	UCL
79643	34	8.31	1.18	1.01	0.03	0.99	0.03	1.46	0.21	NNN	US
79673	83	7.93	0.99	0.98	0.03	1.02	0.03	1.23	0.15	NNN	UCL
79690	70	11.37	1.12	1.00	0.03	0.95	0.03	0.98	0.10	NNN	US
79705	11	1.77	0.78	1.00	0.03	0.97	0.04	1.06	0.46	NNN	UCL
79706	11	19.71	1.29	0.99	0.04	0.95	0.03	0.98	0.07	NNN	US
79710	79	18.19	1.68	1.02	0.03	1.01	0.04	2.19	0.21	NNY	UCL
79733	36	7.87	1.18	0.99	0.03	0.93	0.03	1.29	0.20	NNN	US
79734	42	11.48	1.24	1.00	0.03	0.92	0.03	0.96	0.11	NNN	US
79739	65	14.76	1.11	1.01	0.03	0.95	0.03	1.07	0.09	NNN	US
79742	76	31.67	1.31	1.01	0.03	1.11	0.03	6.08	0.29	NNY	UCL
79771	89	13.01	1.31	1.01	0.03	0.96	0.03	0.97	0.10	NNN	US
79785	77	21.51	1.21	1.03	0.04	0.99	0.04	1.07	0.07	NNN	US
79793	30	4.45	0.95	1.00	0.03	0.95	0.03	0.75	0.16	NNN	US
79794	9	8.41	0.89	0.98	0.03	0.97	0.03	1.01	0.11	NNN	UCL
79806	18	6.61	1.22	1.02	0.03	1.03	0.03	1.04	0.19	NNN	US
79842	15	5.17	0.81	1.00	0.03	0.99	0.03	0.90	0.14	NNN	UCL
79860	72	6.42	0.97	1.06	0.03	1.07	0.03	1.15	0.18	NNN	US
79878	89	34.19	1.61	0.99	0.03	1.25	0.04	2.81	0.15	NYY	US
79897	90	15.13	1.03	1.03	0.03	1.01	0.03	1.16	0.08	NNN	US
79909	36	7.77	1.10	1.01	0.03	0.95	0.03	0.95	0.14	NNN	US
79910	88	8.46	1.08	0.99	0.03	0.96	0.03	0.94	0.12	NNN	US
79977	90	156.40	3.31	1.01	0.03	1.33	0.04	23.28	0.74	NYY	US
79983	46	6.50	0.87	1.02	0.03	1.00	0.03	0.93	0.13	NNN	UCL
80019	27	40.99	3.66	1.04	0.04	1.43	0.06	3.21	0.30	NYY	US
80024	82	65.32	2.41	0.99	0.04	1.07	0.04	3.75	0.18	NNY	US
80036	68	7.56	1.38	0.95	0.02	0.89	0.02	0.94	0.17	NNN	US
80059	84	9.45	0.94	1.01	0.03	0.98	0.03	1.03	0.11	NNN	US
80088	87	26.39	1.36	1.01	0.03	1.14	0.04	3.83	0.22	NNY	US
80089	18	9.67	0.99	0.97	0.03	0.93	0.03	0.98	0.10	NNN	UCL
80108	7	7.48	1.01	1.07	0.03	1.05	0.03	1.22	0.17	NNN	US
80130	89	10.59	1.01	1.04	0.03	0.99	0.03	1.10	0.11	NNN	US
80142	38	16.87	1.88	1.03	0.04	1.01	0.04	0.96	0.11	NNN	UCL
80167	8	19.03	1.07	0.99	0.04	0.95	0.04	0.90	0.06	NNN	UCL
80224	36	15.13	1.45	1.08	0.02	1.05	0.03	1.24	0.12	NNN	US
80238	92	36.50	1.82	1.00	0.04	1.08	0.04	1.81	0.11	NNY	US
80311	86	6.78	1.12	1.02	0.03	0.98	0.03	1.16	0.19	NNN	US
80324	92	10.59	1.53	1.05	0.05	1.09	0.05	0.98	0.15	NNN	US
80371	85	34.76	1.70	1.00	0.04	0.85	0.04	0.97	0.06	NNN	US
80390	79	42.80	1.42	1.12	0.06	0.97	0.05	1.02	0.06	NNN	UCL
80458	49	65.68	1.75	1.02	0.03	1.31	0.04	8.53	0.30	NYY	US

Table 4: The WISE band 4 flux and  $W_2, W_3$  and  $W_4$  flux as a multiple of the photosphere with errors for our sample. <sup>a</sup> This column indicates the detection of an excess in the three colours. The lower section of the table displays the objects removed from our sample due to poor photometry or unreliable images.

HIP	P	$F_{W_4}$ (mJy)	$\sigma_{F_{W_4}}$ (mJy)	$R(W_2)$	$\sigma_{R(W_2)}$	$R(W_3)$	$\sigma_{R(W_3)}$	$R(W_4)$	$\sigma_{R(W_4)}$	Excess <sup>a</sup>	Subgroup
80475	52	22.82	1.13	1.02	0.04	0.96	0.04	0.92	0.06	NNN	US
80493	86	13.51	1.07	1.02	0.04	0.96	0.03	1.00	0.08	NNN	US
80497	26	8.60	1.01	0.99	0.03	1.00	0.03	1.27	0.15	NNN	US
80535	90	10.47	1.15	1.02	0.03	0.96	0.03	0.87	0.10	NNN	US
80582	35	100.15	3.51	1.70	0.10	1.00	0.05	1.03	0.06	NNN	UCL
80591	84	5.82	0.91	0.96	0.03	0.96	0.03	0.86	0.14	NNN	UCL
80711	53	8.76	0.90	1.00	0.03	0.95	0.03	0.97	0.10	NNN	US
80799	91	26.46	2.19	1.02	0.03	1.07	0.04	2.55	0.22	NNY	US
80813	24	12.71	1.11	0.99	0.03	0.97	0.03	1.06	0.10	NNN	UCL
80815	62	78.97	3.20	1.33	0.08	0.96	0.05	1.14	0.08	NNN	US
80851	24	2.23	1.00	1.02	0.03	1.01	0.04	0.74	0.33	NNN	US
80896	86	9.29	1.10	1.01	0.03	0.97	0.03	0.97	0.12	NNN	US
81006	34	6.44	1.41	0.99	0.03	0.97	0.04	0.64	0.14	NNN	UCL
81039	9	12.77	1.19	1.01	0.03	1.00	0.03	1.21	0.12	NNN	UCL
81044	21	8.41	1.24	0.96	0.03	0.90	0.03	0.80	0.12	NNN	UCL
81092	30	15.58	1.11	1.12	0.03	1.06	0.03	0.97	0.07	YNN	UCL
81184	8	3.41	1.19	0.99	0.03	0.96	0.04	1.24	0.44	NNN	US
81208	58	14.76	1.25	0.98	0.04	0.94	0.04	0.91	0.08	NNN	UCL
81266	89	340.28	23.19	1.64	0.14	0.90	0.07	1.14	0.12	NNN	US
81316	41	24.63	1.29	1.04	0.04	1.04	0.04	1.48	0.09	NNY	UCL
81327	6	5.12	1.06	1.00	0.03	0.96	0.03	0.77	0.16	NNN	US
81368	22	16.23	1.11	0.96	0.03	0.92	0.03	1.38	0.10	NNN	UCL
81447	59	13.28	1.15	1.01	0.03	0.99	0.03	1.60	0.14	NNY	UCL
81455	76	6.00	1.24	0.99	0.03	0.96	0.03	1.08	0.22	NNN	US
81472	22	39.50	1.86	1.03	0.05	0.95	0.04	1.15	0.07	NNN	UCL
81477	53	15.54	1.17	0.89	0.02	0.85	0.02	1.02	0.08	NNN	UCL
81582	34	7.65	1.32	1.00	0.03	0.98	0.03	1.32	0.23	NNN	US
81624	79	13836.94	152.93	3.05	0.21	18.34	1.11	72.13	4.33	YYY	US
81692	37	6.78	0.96	0.97	0.03	0.98	0.03	0.83	0.12	NNN	UCL
81751	78	5.43	1.20	1.00	0.03	1.00	0.04	1.29	0.29	NNN	UCL
81772	38	11.10	1.16	1.04	0.03	1.02	0.03	1.07	0.11	NNN	UCL
81887	9	15.95	1.09	1.02	0.04	0.95	0.03	0.86	0.06	NNN	US
81914	58	17.05	3.25	1.03	0.04	0.96	0.04	0.72	0.14	NNN	UCL
81941	44	15.57	1.26	1.00	0.04	0.96	0.03	1.08	0.09	NNN	US
81949	74	15.53	3.37	0.98	0.03	0.99	0.05	1.50	0.33	NNN	UCL
82069	51	37.97	1.50	1.01	0.04	1.13	0.04	2.75	0.13	NNY	US
82154	16	40.09	3.36	0.97	0.03	1.20	0.05	3.28	0.29	NNY	UCL
82187	9	10.41	1.08	1.00	0.03	1.00	0.03	0.99	0.11	NNN	UCL
82208	19	6.95	0.71	0.98	0.03	0.94	0.03	1.01	0.11	NNN	UCL
82218	89	13.74	1.09	0.99	0.03	1.04	0.03	2.05	0.17	NNY	US
82254	16	16.79	1.50	1.05	0.03	1.02	0.03	1.31	0.12	NNN	UCL
82271	12	3.83	1.00	1.01	0.03	1.00	0.03	0.86	0.23	NNN	US
82309	6	5.45	1.17	0.99	0.03	0.94	0.03	0.77	0.17	NNN	UCL
82319	51	4.98	1.19	1.00	0.03	0.97	0.03	0.79	0.19	NNN	US
82397	81	21.21	1.25	0.99	0.03	1.06	0.03	2.07	0.13	NNY	US
82430	78	10.10	1.21	1.02	0.03	0.98	0.03	1.00	0.12	NNN	UCL
82514	65	300.22	6.36	1.74	0.11	0.93	0.05	1.05	0.06	YNN	UCL
82534	89	9.62	1.00	1.00	0.03	0.96	0.03	0.96	0.10	NNN	US
82545	86	144.62	3.33	1.87	0.11	0.98	0.05	0.94	0.05	NNN	UCL
82549	21	3.76	1.24	1.01	0.03	1.00	0.04	1.62	0.53	NNN	UCL
82554	71	18.89	1.11	1.03	0.04	0.99	0.04	1.13	0.08	NNN	UCL
82569	63	6.07	1.26	1.00	0.03	0.93	0.04	0.74	0.15	NNN	UCL
82711	9	28.51	3.86	1.05	0.04	0.98	0.05	1.07	0.15	NNN	UCL
82714	54	97.15	3.04	1.27	0.05	2.80	0.10	4.71	0.21	YYY	UCL
82736	10	4.49	1.18	1.00	0.03	0.95	0.04	1.19	0.31	NNN	US
83061	24	5.46	1.16	1.02	0.03	1.02	0.03	1.06	0.23	NNN	US

Table 4: The WISE band 4 flux and  $W_2, W_3$  and  $W_4$  flux as a multiple of the photosphere with errors for our sample. <sup>a</sup> This column indicates the detection of an excess in the three colours. The lower section of the table displays the objects removed from our sample due to poor photometry or unreliable images.

HIP	P	$F_{W_4}$ (mJy)	$\sigma_{F_{W_4}}$ (mJy)	R( $W_2$ )	$\sigma_{R(W_2)}$	R( $W_3$ )	$\sigma_{R(W_3)}$	R( $W_4$ )	$\sigma_{R(W_4)}$	Excess <sup>a</sup>	Subgroup
83074	11	4.89	1.18	0.99	0.03	0.92	0.03	0.82	0.20	NNN	UCL
83159	62	14.72	1.21	1.00	0.03	1.11	0.04	2.40	0.20	NNY	UCL
83232	11	1141.41	22.08	1.55	0.06	5.87	0.26	38.60	1.48	YYY	UCL
83421	6	1508.83	18.07	1.28	0.04	37.80	1.02	720.22	18.11	YYY	UCL
83457	31	16.53	3.30	1.02	0.04	0.89	0.04	0.74	0.15	NNN	UCL
83460	28	10.91	2.81	0.89	0.03	0.78	0.03	0.95	0.25	NNN	UCL
83508	64	15.20	1.57	1.00	0.03	1.00	0.03	1.00	0.11	NNN	UCL
83611	13	7.46	2.29	0.96	0.03	0.93	0.05	1.00	0.31	NNN	UCL
83637	12	4.16	1.12	0.96	0.03	0.95	0.03	0.87	0.24	NNN	UCL
84222	5	2.09	0.95	0.98	0.03	0.93	0.03	0.53	0.24	NNN	UCL
84267	8	11.37	0.90	0.99	0.03	0.96	0.03	0.89	0.07	NNN	UCL
84473	23	8.92	1.27	0.99	0.03	1.02	0.03	1.31	0.19	NNN	UCL
84565	7	8.74	0.96	1.00	0.03	0.98	0.03	1.14	0.13	NNN	UCL
84593	17	4.65	0.99	0.98	0.03	0.98	0.03	0.94	0.20	NNN	UCL
84605	42	14.85	1.92	1.02	0.04	1.05	0.04	1.17	0.16	NNN	UCL
84657	13	12.24	1.03	0.99	0.03	0.97	0.03	0.93	0.08	NNN	UCL
84766	6	3.94	0.99	0.99	0.03	0.94	0.03	0.52	0.13	NNN	UCL
84881	14	607.91	11.20	1.15	0.04	3.60	0.12	47.93	1.59	YYY	UCL
84931	38	9.75	1.28	0.98	0.04	0.93	0.03	0.82	0.11	NNN	UCL
85278	18	28.75	1.77	1.07	0.05	1.00	0.04	1.06	0.08	NNN	UCL
85316	6	8.84	3.45	0.98	0.03	0.91	0.06	1.74	0.68	NNN	UCL
85389	5	60.96	1.74	1.16	0.07	0.89	0.05	0.99	0.06	YNN	UCL
85478	9	13.94	1.28	0.97	0.03	0.95	0.03	1.33	0.13	NNN	UCL
85663	13	7.89	0.98	0.99	0.03	0.97	0.03	0.87	0.11	NNN	UCL
85700	16	17.81	3.89	1.04	0.04	1.00	0.05	1.04	0.23	NNN	UCL
86010	10	6.99	1.17	0.99	0.03	0.97	0.03	1.05	0.18	NNN	UCL
86098	15	19.60	1.26	0.99	0.04	0.92	0.04	0.81	0.06	NNN	UCL
86134	8	9.88	0.98	1.01	0.03	0.98	0.03	1.00	0.10	NNN	UCL
86853	17	47.63	1.89	1.04	0.03	1.53	0.05	6.07	0.28	YYY	UCL
86903	6	9.81	0.96	0.97	0.03	0.92	0.03	0.98	0.10	NNN	UCL
86922	6	2.26	1.05	0.99	0.03	0.98	0.04	0.74	0.34	NNN	UCL
87042	30	19.10	1.28	0.99	0.04	0.95	0.04	0.86	0.07	NNN	UCL
87198	7	11.74	1.08	0.99	0.03	0.96	0.03	1.10	0.11	NNN	UCL
87337	9	8.97	1.19	0.99	0.03	1.00	0.03	1.13	0.15	NNN	UCL
87924	13	21.10	1.15	1.00	0.04	0.98	0.03	1.12	0.07	NNN	UCL
68413	66	96.97	11.79	1.15	0.05	1.13	0.06	2.02	0.26	YNY	LCC
76063	55	60.23	2.05	1.17	0.06	1.03	0.05	1.40	0.08	YNY	UCL
79098	55	55.65	1.85	1.22	0.06	1.00	0.05	1.40	0.08	YNY	US
77911	83	151.58	3.63	1.05	0.04	1.16	0.04	8.77	0.35	NNY	US

#### Objects removed from the sample due to poor photometry

HIP	P	$F_{W_4}$	$\sigma_{F_{W_4}}$	R( $W_2$ )	$\sigma_{R(W_2)}$	R( $W_3$ )	$\sigma_{R(W_3)}$	R( $W_4$ )	$\sigma_{R(W_4)}$	Excess <sup>a</sup>	Subgroup
50520	62	47.45	1.31	1.16	0.06	0.96	0.05	0.92	0.05	NNN	LCC
50847	62	56.58	1.51	1.30	0.07	1.02	0.05	1.03	0.05	YNN	LCC
52171	8	6.47	0.75	1.23	0.02	0.83	0.02	0.78	0.09	NNN	LCC
52328	7	15.06	0.87	0.46	0.01	0.34	0.01	0.43	0.03	NNN	LCC
52736	25	75.13	2.01	1.27	0.07	0.98	0.05	1.24	0.07	YNN	LCC
54168	13	11.06	0.75	0.98	0.03	0.98	0.03	0.95	0.07	NNN	LCC
54767	64	52.56	1.50	1.33	0.07	1.06	0.05	1.06	0.06	YNN	LCC
55003	6	30.16	1.14	1.09	0.05	1.02	0.04	0.99	0.05	NNN	LCC
55188	78	114.77	3.49	0.91	0.02	1.29	0.03	10.31	0.36	NNN	LCC
55978	18	10.98	1.60	0.99	0.03	0.98	0.05	2.22	0.33	NNN	LCC
56379	83	203910.72	1878.09	2.58	0.13	98.23	4.80	992.09	49.28	NNN	LCC
56673	10	79.33	1.97	1.43	0.08	1.10	0.05	1.25	0.07	YNN	LCC
56943	6	19.73	1.82	0.92	0.02	1.09	0.04	3.24	0.31	NNN	LCC

Table 4: The WISE band 4 flux and  $W_2, W_3$  and  $W_4$  flux as a multiple of the photosphere with errors for our sample. <sup>a</sup> This column indicates the detection of an excess in the three colours. The lower section of the table displays the objects removed from our sample due to poor photometry or unreliable images.

HIP	P	$F_{W_4}$ (mJy)	$\sigma_{F_{W_4}}$ (mJy)	R( $W_2$ )	$\sigma_{R(W_2)}$	R( $W_3$ )	$\sigma_{R(W_3)}$	R( $W_4$ )	$\sigma_{R(W_4)}$	Excess <sup>a</sup>	Subgroup
57451	23	64.78	2.27	1.00	0.04	1.13	0.04	3.25	0.15	NNN	LCC
58326	32	95.20	3.33	0.94	0.04	1.03	0.04	2.88	0.14	NNN	LCC
58528	85	20.19	1.19	1.00	0.03	1.08	0.03	1.82	0.12	NNN	LCC
59360	45	18.55	1.02	1.06	0.04	1.05	0.04	1.01	0.06	NNN	LCC
59413	86	12.19	0.97	0.92	0.03	0.85	0.03	0.77	0.07	NNN	LCC
59781	82	31.67	13.01	0.98	0.03	1.22	0.08	2.92	1.20	NNN	LCC
59898	66	156.26	3.31	1.15	0.05	1.39	0.06	5.09	0.22	NNN	LCC
60718	66	1764.58	30.88	1.75	0.01	1.78	0.01	1.36	0.02	NNN	LCC
61087	88	126.89	4.56	1.11	0.07	2.84	0.18	9.51	0.60	NNN	LCC
62002	49	20.92	1.39	1.06	0.03	1.03	0.03	1.01	0.07	NNN	LCC
62134	83	9.03	0.84	0.77	0.02	0.71	0.02	0.87	0.08	NNN	LCC
62203	15	4.35	0.78	0.98	0.03	0.96	0.03	1.12	0.20	NNN	LCC
63041	83	54.83	17.78	1.02	0.03	1.42	0.10	4.57	1.49	NNN	LCC
63945	79	73.76	2.17	1.28	0.08	0.92	0.05	0.92	0.05	NNN	LCC
64877	61	31.38	1.94	0.88	0.02	0.95	0.03	2.59	0.17	NNN	LCC
64891	17	5.53	0.96	0.97	0.03	0.92	0.03	0.84	0.15	NNN	LCC
65112	81	36.09	1.26	1.15	0.05	1.01	0.04	1.02	0.06	NNN	LCC
65219	78	20.11	1.20	1.05	0.04	1.04	0.04	1.01	0.07	NNN	LCC
65474	26	1511.61	18.10	1.95	0.00	2.04	0.01	1.63	0.02	NNN	UCL
65822	81	16.67	1.01	1.03	0.04	1.01	0.03	0.94	0.06	NNN	LCC
66447	93	25.30	1.14	0.99	0.03	1.04	0.03	2.19	0.12	NNN	UCL
66821	83	111.65	2.47	1.55	0.08	1.06	0.05	1.50	0.07	NNN	LCC
67199	86	27.79	1.07	1.08	0.04	1.05	0.04	1.02	0.05	NNN	LCC
67703	70	51.55	1.61	1.22	0.06	1.00	0.05	1.06	0.06	YNN	UCL
67786	7	71.75	2.25	1.39	0.09	0.93	0.05	0.94	0.06	YNN	UCL
67973	75	45.15	1.46	1.17	0.05	1.13	0.05	1.32	0.07	NNN	UCL
68080	60	64.25	1.89	1.04	0.05	0.99	0.04	1.71	0.09	NNN	UCL
68489	20	7.39	0.87	0.98	0.03	0.96	0.03	1.11	0.13	NNN	UCL
68532	89	14.66	0.89	0.96	0.03	0.94	0.03	0.88	0.06	NNN	UCL
68702	22	2135.21	41.30	6.51	0.03	6.03	0.08	5.47	0.11	NNN	LCC
70518	15	26.03	1.32	1.11	0.05	1.04	0.04	1.03	0.06	NNN	UCL
70765	41	6.85	0.90	1.00	0.03	0.98	0.03	0.90	0.12	NNN	UCL
70918	47	24.40	1.17	1.04	0.04	1.01	0.04	1.04	0.06	NNN	UCL
70931	72	65.32	1.74	1.36	0.09	0.95	0.05	0.93	0.06	YNN	UCL
71353	90	29.97	1.16	1.09	0.05	1.04	0.04	1.03	0.05	NNN	UCL
71856	7	3.48	0.89	1.02	0.03	0.95	0.03	0.88	0.23	NNN	UCL
71860	70	499.62	8.74	0.73	0.01	0.47	0.01	0.44	0.01	NNN	UCL
72216	57	15.40	1.16	1.01	0.03	1.05	0.03	1.49	0.12	NNN	UCL
72685	48	19.19	1.18	0.99	0.03	1.42	0.04	3.46	0.23	NNN	UCL
72984	43	15.73	1.25	0.93	0.03	0.95	0.03	0.88	0.07	NNN	UCL
73150	70	51.65	1.81	1.01	0.04	1.05	0.04	3.04	0.14	NNN	UCL
73937	86	29.10	1.45	1.09	0.05	0.99	0.05	1.01	0.07	NNN	UCL
74321	41	3.60	0.92	0.99	0.03	0.99	0.03	0.85	0.22	NNN	UCL
74950	57	32.32	1.37	1.09	0.05	1.03	0.05	1.02	0.06	NNN	UCL
75151	81	21.41	1.12	0.87	0.04	0.85	0.03	0.84	0.05	NNN	UCL
75843	14	22.11	2.67	1.00	0.03	1.14	0.05	2.37	0.29	NNN	UCL
75915	92	28.46	1.49	1.14	0.04	1.14	0.04	1.22	0.07	NNN	UCL
76126	58	31.23	1.29	1.14	0.05	1.03	0.04	1.00	0.06	NNN	US
76143	51	33.93	1.38	0.90	0.02	1.04	0.03	0.69	0.03	NNN	US
76371	74	73.09	1.88	1.48	0.08	1.04	0.05	1.08	0.05	NNN	UCL
77086	83	39.36	1.38	1.05	0.05	0.93	0.04	0.93	0.05	NNN	UCL
77317	67	32.65	1.44	0.99	0.03	1.11	0.04	3.44	0.18	NNN	UCL
77330	43	9.18	1.02	0.99	0.03	0.96	0.03	0.91	0.10	NNN	UCL
77366	13	7.47	0.98	0.98	0.03	1.04	0.03	1.71	0.23	NNN	US
77399	59	37.59	1.49	1.07	0.04	1.10	0.04	2.19	0.11	NNN	US
77545	84	14.41	1.69	0.99	0.03	1.11	0.04	2.30	0.27	NNN	US

Table 4: The WISE band 4 flux and  $W_2, W_3$  and  $W_4$  flux as a multiple of the photosphere with errors for our sample. <sup>a</sup> This column indicates the detection of an excess in the three colours. The lower section of the table displays the objects removed from our sample due to poor photometry or unreliable images.

HIP	P	$F_{W_4}$ (mJy)	$\sigma_{F_{W_4}}$ (mJy)	R( $W_2$ )	$\sigma_{R(W_2)}$	R( $W_3$ )	$\sigma_{R(W_3)}$	R( $W_4$ )	$\sigma_{R(W_4)}$	Excess <sup>a</sup>	Subgroup
77562	70	164.38	4.54	1.03	0.05	1.30	0.06	4.69	0.23	NNN	UCL
77644	14	5.66	0.91	1.01	0.03	0.75	0.02	0.80	0.13	NNN	UCL
77840	51	234.34	12.09	1.62	0.11	1.11	0.07	2.63	0.21	NNN	US
77858	83	143.43	3.83	1.16	0.07	0.96	0.05	2.33	0.14	YNN	US
78129	22	22.96	1.21	1.04	0.04	1.02	0.04	1.12	0.07	NNN	US
78416	74	9.71	1.20	1.25	0.04	1.22	0.03	1.24	0.16	NNN	UCL
78756	75	18.60	1.03	0.96	0.03	0.97	0.03	1.41	0.09	NNN	UCL
78820	50	596.82	10.44	1.75	0.00	0.95	0.02	1.04	0.02	NNN	US
79031	88	20.19	1.17	1.03	0.04	0.97	0.04	0.97	0.07	NNN	US
79080	51	13153.46	181.72	2.88	0.19	8.88	0.59	23.67	1.58	NNN	UCL
79229	76	27.46	1.31	0.99	0.04	1.00	0.04	1.28	0.08	NNN	US
79230	6	115.62	2.45	1.40	0.06	2.04	0.08	3.65	0.15	NNN	UCL
79363	71	14.28	1.12	0.92	0.03	0.84	0.03	0.79	0.07	NNN	US
79399	82	56.58	1.77	1.12	0.06	0.92	0.05	0.90	0.05	NNN	US
79400	54	19.21	1.15	0.97	0.03	0.93	0.02	1.39	0.09	NNN	UCL
79404	82	161.23	15.30	1.63	0.10	1.22	0.06	2.38	0.25	NNN	US
79476	80	4619.98	46.81	2.54	0.13	28.20	1.20	99.59	3.98	NNN	US
79599	85	22.50	1.51	0.96	0.04	0.92	0.04	0.93	0.07	NNN	US
79622	76	72.75	2.88	1.03	0.05	0.95	0.04	1.92	0.11	NNN	US
79631	86	103.14	2.66	0.94	0.03	1.20	0.04	4.49	0.18	NNN	UCL
80062	57	27.25	4.67	0.96	0.04	0.99	0.05	1.82	0.32	NNN	US
80126	86	215.89	5.77	1.40	0.04	2.74	0.07	12.84	0.44	NNN	US
80208	48	76.39	22.87	1.34	0.08	0.93	0.06	1.43	0.43	NNN	UCL
80425	66	70.38	2.27	1.01	0.03	2.46	0.08	4.94	0.21	NNN	US
80461	81	52.22	2.12	1.38	0.07	1.03	0.05	0.97	0.06	NNN	US
80474	43	45.27	1.75	1.34	0.08	1.49	0.08	1.64	0.10	NNN	US
80557	24	24.70	4.64	0.96	0.03	1.04	0.07	2.18	0.41	NNN	UCL
80569	55	5338.76	103.26	2.73	0.03	5.84	0.07	9.88	0.21	NNN	US
80897	46	97.06	2.23	1.02	0.03	1.95	0.05	14.75	0.46	NNN	UCL
80911	85	263.17	8.73	1.42	0.09	0.99	0.06	2.48	0.15	NNN	UCL
80921	36	7.11	0.96	1.02	0.03	1.03	0.04	2.42	0.33	NNN	UCL
81474	91	239.35	4.85	1.22	0.06	1.29	0.06	5.43	0.25	NNN	US
81589	20	48.60	1.34	1.08	0.05	1.08	0.05	1.22	0.06	NNN	UCL
81639	11	51.17	1.79	1.03	0.05	0.95	0.04	1.51	0.08	NNN	UCL
81791	17	32.80	11.69	0.99	0.04	1.68	0.17	7.05	2.52	NNN	UCL
81891	58	133.61	3.57	0.96	0.04	1.40	0.05	7.27	0.30	NNN	UCL
81972	59	70.90	2.29	1.11	0.05	1.34	0.06	2.01	0.10	NNN	UCL
82091	11	60.12	15.06	0.91	0.03	0.99	0.05	1.84	0.46	NNN	UCL
82250	43	13.14	1.66	1.00	0.03	1.05	0.04	3.49	0.45	NNN	UCL
82663	18	18.44	1.02	0.61	0.01	0.53	0.01	0.52	0.03	NNN	UCL
83321	20	38.00	1.47	1.17	0.06	1.00	0.05	0.90	0.05	NNN	UCL
83535	11	31.26	1.24	1.10	0.05	1.00	0.04	0.99	0.06	NNN	UCL
84445	37	32.83	1.42	1.11	0.04	1.08	0.04	1.37	0.08	NNN	UCL
84673	8	72.08	27.02	1.01	0.04	1.31	0.10	2.91	1.09	NNN	UCL
84734	29	25.96	1.70	0.97	0.04	0.99	0.04	1.30	0.09	NNN	UCL
84888	16	16.50	1.14	1.10	0.03	0.90	0.02	0.91	0.07	NNN	UCL
85927	10	806.57	13.37	3.57	0.02	3.04	0.05	2.30	0.04	NNN	UCL
86670	16	424.85	12.13	1.91	0.06	1.04	0.03	0.98	0.03	NNN	UCL
87948	37	26.24	1.40	1.14	0.05	1.07	0.04	1.04	0.07	NNN	UCL